UNIVERSITA' DEGLI STUDI DI MILANO

SCUOLA DI DOTTORATO DI RICERCA IN SCIENZE BIOCHIMICHE, NUTRIZIONALI E METABOLICHE

DOTTORATO IN BIOCHIMICA

CICLO XXIII

TESI DI DOTTORATO DI RICERCA

NEU4L INDUCES ALTERATIONS ON CELL PROLIFERATION AND DIFFERENTIATION IN NEUROBLASTOMA CELL LINE, SK-N-BE

BIO/10

Federica Cirillo

TUTOR: Prof. re Bruno VENERANDO

COORDINATORE: Prof. re Francesco BONOMI

Ai miei pilastri: Papà, Bassotta e Bimbì (è tutto sotto controllo!!!)

INDEX

CHAPTER I

SIALIDASES

1.1 SIALIDASES

Sialidases or neuraminidases constitute a family of exoglycosidases that catalyze the hydrolytic cleavage of nonreducing sialic acid residues ketositically linked to mono- or oligosaccharide chains of glycoconjugates.

The terms "sialidase" and "neuraminidase" have been proposed for the first time by Heimer and Meyer (1956) and Gottschalk (1957), respectively; the first name is used to indicate the eukaryotic enzyme, while the second to indicate the bacterial and viral counterparts.

Sialic acid is present in sialoglycoconjugates as a terminal non-reducing residue usually linked to galactose ($\alpha 2 \rightarrow 3$ or $\alpha 2 \rightarrow 6$), and to N-acetylgalactosamine or N-acetylglucosamine ($\alpha 2 \rightarrow 6$); moreover, the sialic acid chains may be present as terminals, or wire internal saccharide residues into glycolipids and glycoproteins. The formation of co-polymers of sialic acid through links ($\alpha 2 \rightarrow 8$ or $\alpha 2 \rightarrow 9$) can also be found. Sialidases preferentially recognize the link $\alpha 2 \rightarrow 3$ or $\alpha 2 \rightarrow 6$, while in some cases also hydrolyze bonds $\alpha 2 \rightarrow 8$; internal residues are resistant to hydrolysis by these enzymes, probably due to the steric hindrance.

Sialidases are widely distributed in nature, from viruses, and microorganisms such bacteria, protozoa and fungi to avian and mammalian species among the vertebrates.

Perhaps, the most widely studied sialidase is from influenza virus, where the enzyme is involved in viral replication and is released from infected cells (1, 2).

In bacteria sialidases are not only involved in infection processes, but also in cellular energy supplying: in fact, the enzymes hydrolyze sialic acid residues from mucins and gangliosides, making available new carbon for energy purposes (3).

The detailed study of mammalian sialidases has been hampered for a long time because of their low cellular concentration and thermal liability during the classic purification procedures.

The turning point came with the advent of molecular biology, which allowed to give a great impetus to this field of study.

In mammals, these enzymes have been proved to be involved in several cellular phenomena, including cell proliferation and differentiation, membrane functions, and antigen masking (1).

1.2 HUMAN SIALIDASES

The presence of sialidase activity was detected in all human cells and tissues. In human, four isoforms have been described and distinguished on the basis of different intracellular localization and substrate specificity.

The classification identifies:

1) The sialidase Neu1 localized in lysosomes
2) The sialidase Neu2 localized in the cytoplasm
3) The sialidase Neu3 localized on the plasma membrane
4) The sialidase Neu4 localized on the outer mitochondrial membrane and on inner cell membrane

The lysosomal sialidase, Neu1, is involved in the catabolism of glycoproteins, glycolipids and oligosaccharides, in combination with lysosomal proteases and endoglycosidases, since different substrates must be fragmented into small molecules before desialylation (4).

The intracellular distribution of Neu1 depends on the last four amino acids (412-YGTL-415) of the polypeptide, which address the enzyme to lysosome. Beside this main localization, Neu1 could also detected on the plasma membrane in several cell types. Further to T lymphocytes activation, the sialidase activity detected on the cell surface increase several times due to the redistribution of Neu1 from the lysosomes to the plasma membrane. This enhancement of sialidase levels is required for both early production of IL-4 and the linfokine priming of conventional T cells to became active IL-4 producers(1). In addition, redistribution of Neu1 from lysosomes to the plasma membrane of activated lymphocytes is associated with tyrosine phosphorylation of the enzyme (5). In this prospective, the interaction of Neu1 with adaptor complexes such as AP2 and AP3 (6, 7), and targeting to the lysosome should be blocked by phosphorylation of the essential tyrosine (Y^{415}) in the internalization signal, a mechanism already described for cytotoxic T-lymphocyte-associated antigen (CLTA-4) (8).

The movement of the enzyme induces the desialylation of molecules expressed on the membrane surface, as the antigen class I Major Histocompatibility Complex (MHCI) and the ganglioside GM3. This is a process linked to the synthesis of IL-4 (1).

Moreover, in activated T lymphocytes Neu1 contributes to small desialylation processes which induce the synthesis of IFN-γ (9), whereas in activated B cells the sialidase Neu1 is involved in the production of the so-called MAF (macrophage activating factor) (10). These events explain the responsiveness towards the "antigen presenting cells"; the production of IL-4 or MAF is strongly compromised in immune cells with a deficiency of sialidase activity (10). Moreover, the enzymatic defect accounts for the frequent infections observed in patients with sialidosis.

During the activation of neutrophils, a same mechanism for redistributing of Neu1 sialidase from lysosomes to the plasma membrane has been described (11). This event is followed up by the removing sialic acid from glycoconjugates on the surface of the cell and the activation of non-activated adjacent cell. This mechanism induces an increased of aggregation and adhesion to the substrate, a key function in diapedesis (11).

The lysosomal sialidase is an enzyme essentially ubiquitous, with particularly high levels of expression in pancreas, skeletal muscle, kidney, heart, placenta, liver, lungs and brain (12).

Several NEU1 gene mutations underlie a severe lysosomal storage diseases: the sialidosis (12).

In mammalian tissues, Neu1 is present as a high-molecular-weight multienzyme complex with the protective protein/cathepsin A (PPCA) and β-galactosidase (2) and co-purifies with these proteins (13, 14).

The high molecular weight of the complex is due to the formation of polymers of these multiproteins units. The role of this complex is the protection of the enzymes from the lysosomal proteases and the stabilization of their activity (15).

Lysosomal sialidase has been extensively investigated as a target gene for sialidosis. Sialidosis patients carry mutations in genomic DNA coding for NEU1, including frameshift insertions and missense mutations (16).

Genetic defects of the PPCA protein cause the rapid degradation of both sialidase and β-galactosidase and are associated with another serious disease lysosomal storage: the β-galactosialidosis (15).

Instead, galactosialidosis is an autosomal, recessively inherited, lysosomal storage disease (17).

Like sialidosis, patients with galactosialidosis also accumulate and excrete large amounts of a complex carbohydrate mixture of glycopeptides fragments rich in sialic acid (18).

In galactosialidosis, there is a combined deficiency of sialidase and β-galactosidase (18).

In fibroblasts of galactosialidosis patients, the levels of both sialidase and β-galactosidase are severely deficient compared to the levels present in normal fibroblasts (19). The deamidase and carboxypeptidase activity associate with the "protective protein" is also deficient in galactosialidosis (20).

In both these pathological diseases there are neurological signs as cherry-red spots, myoclonus, and mental retardation. Moreover, there are skeletal dysplasia, corneal clouding, hepato-splenomegaly, hernia, coarse face, and hearing loss. Foam cells appear in the bone narrow. Endothelial cells and lymphocytes are vacuolated (21).

The cytosolic sialidase Neu2 is unique among sialidases to not provide trans-membrane domains (22), but has a cytosolic distribution. This enzyme is characterized by broad substrate specificity, being capable of hydrolyzing sialic acid residues from glycoproteins, gangliosides and oligosaccharides.

Studies demonstrated that, during myoblast differentiation, NEU2 mRNA levels as well as enzyme-specific activity increase, and myo-tube formation can be blocked by the addition of specific antisense oligomers (23).

The enhancer/promoter sequence of rat cytosolic sialidase contains four E-boxes and a classic TATA box. E-boxes are involved in the development and tissue-specific regulation of muscle gene transcription (24).

A similar organization of 5'-upstream region is reported from human NEU2 gene (22), indicating that at least the rat and the human gene are preferentially expressed in muscle tissue. In addition, the rat 5'-upstream region is better characterized following its ability to drive the transcription of a reported gene in transient transfection experiment (25).

The promoter region is active in rat myogenic cells, and its transcriptional activity is increased after induction of myoblast differentiation. Further studies demonstrated that during myoblast differentiation NEU2 mRNA levels as well as enzyme-specific activity increase, and myotube formation can be blocked by addiction of a specific antisense oligomer (23). Finally the enzyme appears to be diffusely distributed in the muscle

fibers and also found in the perimysium and blood vassels. In addition, many immunogold particles are also found in the cytosolic compartment of axons, Schwann cells, and cells of endomysium and again, blood vassels, indicating that Neu2 is also present in cells other that skeletal muscle fibers (26).

Many results confirm the participation of Neu2 in the process of muscle differentiation (27) and in cell motility (28).

Among the sialidases, Neu3 is a key enzyme for ganglioside degradation because of its strict substrate preference to gangliosides, which co-localize with this sialidase in the surface membranes (2). Neu3 expression has been found to fluctuate with cell differentiation, cell growth, and malignant transformation (2).

Recent analysis of membrane topology has suggested that Neu3 might be partially localized on the cell surface as peripheral membrane protein and also in the endosomal compartment (29). In addition, Neu3 cofractionates with markers of lipid rafts (30), membrane functional microdomains where gangliosides and other glycosphingolipids are arranged together with signaling proteins (31). Among these compounds, gangliosides are the most abundant in the plasma membrane of vertebrate cells and are involved in several important biological processes (32).

In human neuroblastoma cells, Neu3 specifically acts on gangliosides with terminal sialic acid, yielding to GM1 and lactosylceramide, and its action on glycolipids is necessary and sufficient to trigger differentiation in this kind of cells (33).

Neu3 also functions as a caveolin-interacting protein within caveolin-rich microdomains via a putative caveolin-binding motif within the molecule (34).

Neu3 expression is shown to participate in neuronal differentiation through gangliosides modulation (35), as the murine homolog gene is shown to play essential role in neurite formation (36) and regeneration (37). A massive desialylation of the cell surface carried out by endogenous as well exogenous sialidases has been suggested as critical event for myelination (38), neuronal differentiation (33, 39, 40), synaptogenesis, and synaptic function (41, 42). Moreover, it has been demonstrated the involvement of sialidase Neu3 during the formation of axons in rat: the enzyme enhances the activity of the TrkA receptor, which, in turn, mediates the response to NGF (43).

High expression of NEU3 in cancer cells leads to protection against programmed cell death; while in contrast, decreased NEU3 induces apoptosis, implying a critical role of Neu3 in the survival of cancer cells (44).

Several studies have shown that the participation of Neu3, in the events downstream of insulin-receptor interaction, occurs through the desialylation of membrane gangliosides and through a direct link between Neu3 and GRB2 signal protein. The ability of sialidase to regulate the cellular response induced by insulin may explain the altered expression levels of sialidase in insulin-dependent diabetes types II (45).

Furthermore the over-expression of NEU3 in vascular smooth muscle cells induces a decrease in metallo-protease 9 in response to TNF α, suggesting that Neu3 is a physiological modulator in these cells and may contribute to the instability of atherosclerotic plaques (46). Neu3 is probably involved in cell-cell interactions though hydrolyzing the gangliosides localized on the surface of neighboring cell (47).

The most recently identified member of the human sialidase family is Neu4 and it is found in two forms, Neu4 long (Neu4L) and Neu4 short (Neu4S), differing in the presence of a 12-amino-acid sequence at the N-terminus (48, 49).

The expression of the isoforms is tissue specific; both isoforms were expressed in the brain, muscle, and kidney, and predominantly the short form was expressed in liver and colon.

It has been observed that the presence of Neu4S could help the elimination of the sialylated products, accumulated in lysosomes; therefore, Neu4S could be seen as a possible target for the development of new treatments in diseases such as sialidosis and galactosialidosis where lacking sialidase Neu1 is lacking (12).

Although the physiological roles of Neu4L in brain still remain elusive, its substrate specificity and subcellular localization suggest that it may be implicated in the mitochondrial apoptotic pathway in neuronal cell. Given its unique location, in mitochondria, Neu4L is believed to be involved in apoptosis by regulating the levels of mitochondrial, hydrolyzing ganglioside GD3 (50).

Recently, it is demonstrated that Thymoquinone (TQ), from nutraceutical black cumin oil, activates Neu4 sialidase in live macrophage, dendritic, and normal and type I sialidosis human fibroblast cells via GPCR Gαi proteins and matrix metalloproteinase.

The activation of this pathway induces the production of NF-KB and pro-infiammatory cytokines in vivo (51, 52).

1.3 GENE STRUCTURE

The human gene NEU1 spans about 3.7 kb of DNA on chromosome 6p21.3 and is organized in six exons (53) (Fig.1).

The cDNA encodes a protein of 415 amino acids with an Arg-Ileu-Pro sequence, five Asp boxes and as potential N-linked glycosylation site. The molecular weight of Neu1 is 45.5 kDa (4).

The human gene NEU2 has a very simple organization. In fact, the gene is organized in two exons separated by one intron on chromosome 2q37.1 (22) (Fig.1). The promoter region contains a classic TATA box and four E-boxes (54) that are described as the DNA binding motif recognized by several nuclear factors belonging to the basic helix-loop-helix family of DNA binding protein. The cDNA encodes a protein of 380 amino acids with. Molecular weight of Neu2 is 42.8 kDa (22).

The human gene NEU3 contains four exons and is located on chromosome 11q13.4 (55).

Sequence analysis of the 5' untranslated region reveals the presence of several Sp1-binding sites and the absence of TATA and CAAT box sequences, in agreement with northern blot analysis that shows a ubiquitous expression pattern.

The NEU4 gene is apparently organized in four exons in a region of chromosome 2q37.3 (Fig.1). The codon for the translation-initiator methionine is located in exon 2, whereas the terminator codon, TAA, is located in exon 4. The predicted Neu4 protein is 484 amino acids long, with a calculated molecular weight and theoretical pI of 51.57 kDa and 7.97, respectively. The sequence motif F/YRIP which is highly conserved in all of the sialidase enzymes and occurs near the N-terminus of these polypeptides, is also found in Neu4 with a V residue instead of canonical I. Moreover, NEU4 contains two classic Asp blocks, both in agreement with the consensus sequence. A characteristic feature of Neu4 is a long stretch of 79 amino acid residues that appears unique among mammalian sialidases (49).

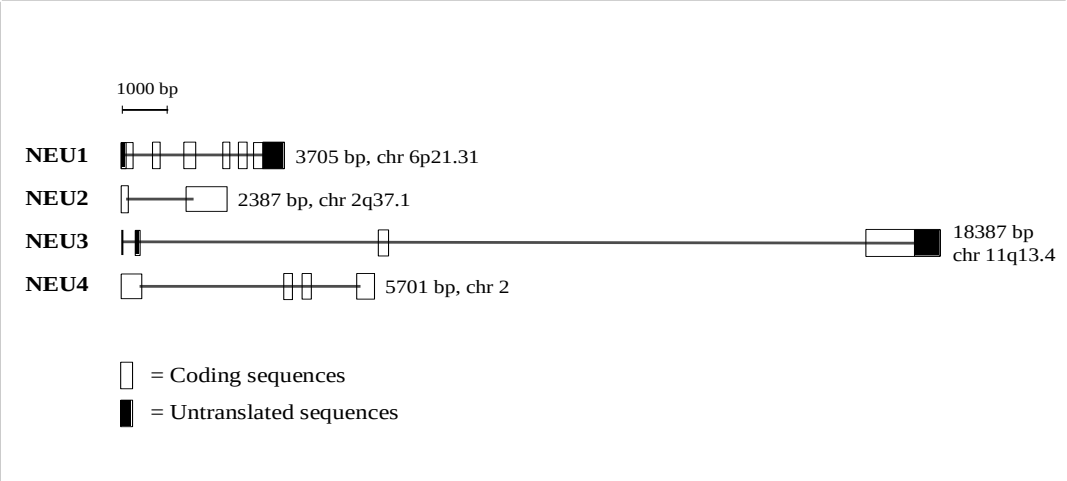

Figure 1: genic structure of human sialidases NEU1, NEU2, NEU3, NEU4

1.4 MOLECULAR BIOLOGY OF HUMAN SIALIDASES

The molecular biology of sialidases began in 1993 when the first mammal sialidase was cloned: the cytosolic sialidase in rat skeletal muscle (56).

The analysis of the primary structure of protein has demonstrated significant homology with microbial enzymes: in particular, characteristics have been identified sequences such as the domain F(Y)RIP, at the amino-terminal portion of the enzymes, and a series of so-called Asp-boxes (SxDxGxxT/W), repeated several times in the protein sequence (57, 58).

During the following year, cDNA encoding a soluble sialidase was cloned. It was secreted into the growth medium from hamster ovary (57).

We must wait for the late 90s for the first cloning of the human lysosomal enzyme, NEU1 (4).

In 1999, using an approach based on sequence homologies, the gene NEU2 was identified (22), encoding the human cytosolic sialidase; this enzyme has been found very similar to the counterparts of rat and hamster cloned in previous years.

In the same years the gene encoding sialidase NEU3 membrane was also identified (55, 59).

In 2004, the fourth gene encoding the human sialidase NEU4 was identified (49).

All mammalian sialidases cloned show a high degree of homology and the presence of amino acid residues substantially preserved: the sequence motif F(Y)RIP and the Asp

boxes, in topologically equivalent positions along the primary structure. The role of the Asp box is not yet known, although it was suggested an involvement in the folding of the enzymes and in maintaining the structure of the catalytic domain. Instead, the sequence F(Y)RIP, located in amino-terminal position, gives an arginine to the catalytic triad of residues that interacts with the sialic acid carboxyl group during the stages of substrate binding and catalysis (60).

In addition, other 8-9 residues of the bacterial sialidase were found also in mammalian sialidases. This shows as the evolutionary pressure has maintained a consistent level of conservation, particularly near the catalytic site.

The level of similarity between sialidases from different species reaches 75%, if we group the different sequences of sialidase according to their cellular localization.

For these reasons, some evolutionary hypotheses indicate the possible existence of a common ancestral gene from which they took home all the currently known isoforms (61).

1.5 SIALIDASES AND CANCER

Given the importance of the glycosylation profile in the neoplastic cell, for many years the interest has been focused on these enzymes that regulate the carbohydrate structure of proteins and lipids; indeed, the abnormal glycosylation processes are a common sign of cancer (62). Investigation into biochemical properties of the cell surface were extensively pursued and characteristic features of the changes in cancer cells were identified (62).

The changes of glycosylation in glycoproteins include an increase in branched asparagines-linked and polylactosamine sugar chains, as well as, in sialylation (63). In particular, alteration of sialic acids is associated with cancer behavior, such as invasiveness and metastasis (63). Altered glycosylation of functionally important membrane glycoproteins may affect on the adhesion or motility of the tumour cells, resulting in invasion and metastasis. Specifically, abnormalities of membrane glycoproteins, such as selectins and integrins, influence in the adhesion properties and motility of cancer cells, inducing consequences on the growth and the metastatic potential of tumour (64).

Moreover, an altered sialylation of glycolipids (65) is also observed as a ubiquitous phenotype, leading to the appearance of tumour-associated antigens, aberrant adhesion, and modification of transmembrane signaling (66).

Cancer cells are characterized by the presence of antigen-specific glycosphingolipids, often absent in healthy cells (67). These molecules, especially gangliosides, are shed into the surrounding microenvironment in higher volumes than healthy tissue (67). The tumour gangliosides on the cell membrane or secreted appear to play keys role in disease progression; in fact, they strongly regulate the adhesion/cell motility by participating actively in the metastatic processes (67). Moreover, these gangliosides may act as immuno-suppressants, may promote angiogenesis by stimulating the release of VEGF and may modulate signal transduction through interaction with receptors for growth factors (68).

To understand the causes of aberrant sialylation and the consequences of these changes, the studies have been focused on mammalian sialidases which control the cellular sialic acid content, in cooperation with sialyltransferases.

Scarce evidences are still available on sialyltransferases and on their involvement in neoplastic transformation; on the contrary, characteristic changes in the expression and activity of sialidases have been revealed in different tumour types.

The lysosomal sialidase activity (Neu1) decreases in rat 3Y1 fibroblasts after src-transformation. NEU1 expression has been found to be inversely correlated with the metastatic potential of the cells (69). As compared to mock 3Y1 cells, src-transformed cells exhibited decrease of Neu1, and v-fos transfer to these cells induce an even more severe decrease in sialidase activity with the acquisition of high lung metastatic ability (69).

The transfection of murine lysosomal sialidase, into B16 melanoma cells, causes the suppression of tumour progression (70). Transfection of NEU1 reduces cell growth and anchorage-independent growth and increases the sensitivity to apoptosis, induced by suspension culture or serum depletion in vivo (70).

The levels of NEU1 expression have been evaluated in human colon cancer. Its mRNA level shows a tendency toward decrease in cancer cells as compared to those in the adjacent noncancerous mucosa (36). NEU1 over-expression results in alterations similar

to those observed in murine cells; in fact, in human colon adenocarcinoma HT-29 cells it suppresses cell migration and invasion (68).

The suppression of pulmonary metastasis in murine B16 melanoma cells has been obtained by transfection with NEU2 cDNA (28). Surprisingly, this change in the highly invasive and metastatic behavior of the cells appears to be related to variations of intracellular glycolipids levels. In fact, upon NEU2 transfection, the major detectable changes were the increase of lactosylceramide and the decrease of ganglioside GM3 cell content. The GM3 ganglioside has been found associated with microtubules and intermediates filaments inside the cell (71). Thus Neu2 could act on intracellular GM3, leading to alteration of cytoskeletal functions consistent with the decrease of invasiveness detected in transfected melanoma cells.

Similar results were obtained using highly metastatic sub-lines of mouse colon adenocarcinoma 26 (68). Also, in these malignant cells, endogenous Neu2 sialidase levels are inversely correlated with the metastatic capacities. These modifications are correlated with sialylLe^x and GM3 cellular levels.

Another line of the experiments performed employing the cytosolic sialidase demonstrated that the transfection of NEU2 gene into the epidermoid carcinoma line A431 reduces the GM3 levels and enhances cell growth and tyrosine autophosphorylation of EGF receptor at low EGF concentration (72).

NEU2 transfection into the chronic myelogenous leukemia cells K562, which are devoid of cytosolic sialidase activity, induces a significant decrease in resistance to apoptosis, possibly mediated by modifications of the interaction between cytosolic sialoglycoproteins and on the signaling pathway of Bcr-Abl and Src kinases (73).

Many data identified Neu3 as a new oncogene, given its involvement in tumorigenesis (74). Tumors usually express a characteristic up-regulation of Neu3 (75).

In particular, the mRNA NEU3 levels resulted to be increased in all colon cancer tissue surgical specimens as compared with that in adjacent noncancerous mucosa (36).

Colon cancer tissue specimens exhibit marked accumulation of lactosylceramide, a possible Neu3 product; the addition of this glycolipid to the culture medium reduces the number of apoptotic cells during sodium butyrate treatment (36). These results indicate that the high contain of Neu3 in cancer cells leads to the protection against programmed cell death, through the increase of lactosylceramide while, in contrast, the decrease of

Neu3 induces apoptosis, implying a critical role of Neu3 in the survival of cancer cells. It is of interest to note here that while Neu3 silencing caused acceleration of apoptosis in various cancer cells, it has been shown not to have the same effect in noncancerous cells, including human normal keratinocytes and fibroblasts (36).

NEU3 mRNA levels were also found to be increased in renal cell carcinomas as compared with those adjacent non cancerous tissues (36),being significantly correlated with the elevation of expression of interleukin (IL)-6, a pleiotropic cytokine, which has been implicated in the immune responses and in the pathogenesis of several cancers

NEU3 activated by IL-6, in turn, enhances exerts IL-6 mediated signaling largely via the PI3K/Akt cascade, in a positive feedback manner and contributes to the expression of the malignant phenotype in renal cancer (76).

Transfection of NEU3 gene into cancer cells inhibits apoptosis through the increase of Bcl-2 and the decrease of caspase expression, while the silencing of this gene with short-interfering RNA results in acceleration of apoptosis (77).

In prostate cancer cells up-regulation of Neu3 leads to the suppression of cell differentiation and apoptosis, and thus may be related to malignant properties (36).

Furthermore, in head and neck cancer (36), in most ovarian clear cell adenocarcinoma (78), in chronic myeloid leukemia cells (79) Neu3 is increased.

In particular, in chronic myeloid leukemia cells K562, NEU3 silencing markedly modifies the cell cycle, reducing proliferation rate; moreover, it causes a propensity to undergo apoptosis, and megakaryocytic differentiation (76).

In clear contrast to Neu3, a marked decrease of NEU4S expression is detected in tumour as compared with noncancerous cells (80).

In cultured human colon cancer cells, the enzyme is up-regulated in the early stage of apoptosis induced by either the death ligand TRAIL, or serum depletion (36).

Transfection of NEU4S into DLD-1 and HT-15 colon adenocarcinoma cells results in the acceleration of apoptosis and in the decrease of invasiveness and cellular motility. On the other hand, siRNA-mediated NEU4 targeting causes a significant inhibition of apoptosis and promotion of cellular invasiveness and motility (36).

Neu4S plays important roles in the maintenance of normal mucosa, mostly through desialylation of the glycoproteins and its down-regulation may contribute to the invasive properties and protection against programmed cell death of colon cancer (36).

The short isoform is localized on the internal cell membranes. Studies have been performed on fibroblasts of patients with sialidosis and galactosialidosis diseases. In these works, Neu4 short is over-expressed and there was a greater digestion of gangliosides deposited in lysosomes (81). This suggests a potential treatment of diseases caused by defects in the gene NEU1.

For Neu4L, involvement is hypothesized in regulating the mitochondrial pathway of apoptosis induction. This role is particularly relevant to the nervous system where it is particularly expressed sialidase; SH-S5SYcells is observed that following induction with tyrosinase there is a decrease of the enzyme and an associated increase in GD3 (50). A marked decrease of NEU4S expression was detected in tumours as compared with in the noncancerous mucosa (80).

In mouse neuroblastoma cells, Neuro2a, NEU4 expression is down-regulated during retinoic acid-induced differentiation. Over-expression of Neu4 results in suppression of neurite formation, and its knockdown showed the acceleration (82).

CHAPTER II

NEUROBLASTOMA

2.1NEUROBLASTOMA

Neuroblastomas are neuro-ectodermal tumours of embryonic neural crest-derived cells (83). In normal development the neural crest gives rise to nerve cells of sympathetic nervous system. This is formed by sympathetic chains and ganglia, which run alongside the ventral side of spine, and adrenal medulla (83, 84). The fetal adrenal medulla consists of a mixture of chromaffin cells and clusters of mature ganglioside cells (83, 84).

Chromaffin cells are neuro-endocrine cells and produce the stress hormones norepinephrin and epinephrine. Ganglion cells are nerve cells interconnected between pre- and postganglionic fibers of sympathetic nervous system. The amount of chromaffin cells in adrenal medulla strongly increases after birth, in concert with a gradual loss of ganglion cells (84). In the extra-medullary sympathetic nervous system, the opposite can be observed: extra-medullary chromaffin cells will rapidly disappear from ganglia, and the neural cells become the predominant cell type (84, 85).

Neuroblastoma likely originates from both the cell types, described above, or from a pluripotent precursor cell, since the tumor can contain cells with neuronal and chromaffin cell properties (84, 85, 86).

Neuroblastomas are undifferentiated tumours, constiting of small, round cell called neuroblasts that have little evidence of neural differentiation. However, some tumours show partial histological differentiation and are called ganglioneuroblastomas (86).

Ganglioneuroma consists of clusters of mature neurons surrounded by a dense stroma of Schwann cells (86) and, in general, has a favorable prognosis.

Neuroblastoma is the third most common pediatric cancer and is responsible for approximately 15% of all childhood cancer deaths (87), and 96% of cases occur before of 10 years (88).

The clinical hallmark of neuroblastoma is heterogeneity, with the likelihood of tumour progression varying widely according to anatomic stage and age at diagnosis (89).

In general, children diagnosed before 1 year of age and/or with localized disease are curable with surgery and little or no adjuvant therapy. Some of these tumours undergo spontaneous regression or differentiate into benign ganglioneuromas (89).

In contrast, older children often have extensive hematogenous metastases at diagnosis, and the majority dies from disease progression despite intensive multimodal therapy (89).

Patients usually can be classified as high, intermediate or low risk. High risk tumours include disseminated disease or bulky tumours with some specific genetic alterations, such as the amplification of oncogene N-myc. These patients form a group at risk with a 5-years event-free survival (EFS) of 25/30% despite multi-modality treatment including myelo-ablative chemotherapy (90).

Patients with intermediate risk disease are characterized by large, unresectable, localized tumours without structural chromosomal defects. Their outcome is more favorable (5-years EFS of 60-80%) and can be reached by combining surgery with adjuvant chemotherapy (90).

Low risk tumours include children which can be managed by surgery alone and will lead to an excellent 5-years EFS of more than 90% (90).

The aetiology of neuroblastoma is unknown, but it seems unlikely that environmental exposures have a significant role (91).

2.2 SEVERAL KINDS OF PHENOTYPES IN NEUROBLASTOMA CELL LINES

The initial morphological identification of cellular phenotypes present in human neuroblastoma cell lines identifies two phenotypically stable cell variants: a neuroblastic (N-type) cell and a flattened, substrate-adherent (S-type) cell (92-95).

N cells are, usually, small and weakly substrate-adherent. They frequently have small neurites and grow as clumps of cells (pseudoganglia) or floating balls (93-95).

S cells adhere tightly to the underlying substrate, form a contact-inhibited monolayer, and have a limited lifespan in culture (93-95).

A third stable cell type was subsequently identified and is similar, yet distinct, from the other two cell types. It was called “I-type” at its discovery because its morphological and growth characteristics are “intermediate” between N- and S-type cells; it was soon recognized to be a malignant neuroblastoma stem-like cell type by its unique differentiation and malignant potentials (96, 97).

Biochemical and immunochemical studies confirm the sympathoblastic nature of the N cells and identify the S-type cells as precursors of the non-neuronal component of the embryonic neural crest such as Schwann cells, melanocytes, and smooth muscle cells (97-99).

However, neither N nor S cells usually express marker proteins characteristic of late-stage development; the absence of markers of mature neurons or non-neuronal neural crest derivatives revealed the less differentiated nature of the cells (97-99).

Consistent with their morphological features, the I-type cells, typically, express marker proteins of both N and S cell lineages.

Whereas all three cell variants express the intermediate filament nestin, characteristic of early neuroepithelial cells, only I-type cells, and not their N or S cell counterparts, express the stem cell marker proteins CD133 and c-kit (100, 101).

2.3 GENETICS OF NEUROBLASTOMA: NEAR-DIPLOIDY VERSUS NEAR TRIPLOIDY AND AMPLIFICATION OF NMYC

Somatic changes, such as gain of alleles and activation oncogenes, loss of alleles or changes in tumour-cell ploidy have been shown to be important in the development of sporadic neuroblastomas.

Although tumours have karyotypes in the diploid range, tumours from patients at lower stages of disease are often hyperdiploid or near-triploid (102, 103).

It has been shown that the determination on the ploidy status content of neuroblastoma in infants can be predictive of outcome (104, 105).

In patients older than 2 years, ploidy loses its prognostic significance (105). This is probably because hyperdiploid and near-triploid tumours in infants, generally, have gains of whole chromosome without structural rearrangements, whereas tumours in older patients also have several structure rearrangements.

Some neuroblastomas are cytogenetically characterized by double-minute chromatin bodies (DMs) or homogeneously staining regions (HSRs), which are both cytogenetic manifestations of gene amplification. In neuroblastoma, it has been found a novel MYC-related oncogene, NMYC, which is frequently amplified (106).

NMYC is normally located on the distal short arm of chromosome 2; a large region from chromosome 2 amplified, maybe because it provides some selective advantage to the cells (91).

The process of amplification usually results in 50 to 400 copies of the gene per cell, with, correspondingly, higher levels of protein expression (107). Intermediate copy levels numbers (three to ten copies) may reflect either low-level amplification or aneuploidy.

It was shown that NMYC amplification occurs in a substantial subset of primary untreated neuroblastomas and is highly correlated with an advantage stage (108). Moreover there is a strong association with rapid disease progression and poor prognosis (109).

Subsequent investigations have confirmed that, when NMYC gene amplification is bigger than ten copies, the prognostic powerful is independent of anatomic stage, age, and multiple other biologic measures.

NMYC is a proto-oncogene normally expressed in the developing nervous system and selected other tissues. The NMYC gene product, NMyc, is a nuclear phosphoprotein with a short half-life and regions of marked similarity to c-myc (110). NMyc must first dimerize to Max to activate transcription (111).

Max is a ubiquitously expressed nuclear protein with a long half-life, that lacks the amino-terminal trans-activation domain which characterizes the Myc protein family. The formation of the heterodimer Max/NMyc leads to the transcriptional activation of an as yet undefined series of growth-promoting genes (89). Even though NMYC has a short half-life, the extremely high steady-state levels in amplified tumour cells probably ensures that cells stay in cycle and do not enter G0 (112).

Some neuroblastoma cell lines express high levels of NMYC mRNA or NMYC protein without gene amplification (107, 113), perhaps due to alterations in normal protein degradative pathways rather than loss of NMYC transcriptional auto-regulation (114, 115).

A strong correlation between NMYC amplification and 1p loss of heterozygosity (LOH) has been shown (116). Both NMYC amplification and deletion of chromosome 1p are strongly correlated with a poor outcome. Most cases with NMYC amplification also present 1p LOH, but not all cases with 1p LOH have NMYC amplification, indicating

that 1p deletion might precede the development of amplification. Indeed, it might be necessary to delete a gene that regulates NMYC expression, or one that mediates programmed cell death in the presence of high NMYC expression. Alternatively, there might be an underlying genetic abnormality that leads to genomic instability that predisposes to both 1p LOH and NMYC amplification (91).

The targets of NMYC remain mostly unknown. Among the most important identified so far is MDM2, an inhibitor of p53, which causes the translocation of p53 from the nucleus to the cytoplasm through a nuclear export signal (117).

In neuroblastomas with NMYC amplification, there is an increase of MDM2 with decreased activity of p53 and therefore a resistance to apoptosis of cells and the tendency to proliferation.

2.4 EXPRESSION OF NEUROTROPHIN RECEPTORS

The study of neurotrophins during the neoplastic transformation has become interesting because of the central role of neurotrophin signaling in normal neuronal development. Neurotrophins are critical to the development of sympathetic nervous system as nerve growth factor (NGF), brain-derived neurotrophic factor (BDNF), neurotrophin-3 and neurotrophin-4. Neurotrophin signaling is mainly mediated through the Trk family of tyrosine kinases. To date, three high-affinity neurotrophin receptor genes relevant to neuroblastoma have been cloned: TRKA, TRKB and TRKC, and their expression is developmental regulated (91).

TrkA is a transmembrane receptor that, probably, acts as a homodimer. Binding of TrkA to an homodimer of NGF activates the autophosphorylation of receptor, the docking of signaling proteins and induces gene transcription. Activation of specific signaling pathways has been linked to survival and to differentiation, whereas inhibition of TrkA activation can lead to programmed cell death, depending in part on the state of differentiation of the cell. So, the presence or the absence of NGF can have a profound effect in cellular behavior (91).

High levels of TrkA expression are correlated with younger age, lower stage and absence of NMYC amplification. TrkA expression is highly correlated with a favorable

outcome, and the combination of TrkA expression and NMYC amplification provides even greater prognostic power (91).

TrkA/NGF pathway might have an important role in the propensity of some neuroblastomas to differentiate or to lead to programmed cell death (91). In contrast, full-length TrkB is expressed preferentially in advanced stage, NMYC amplified neuroblastomas (118). Many of these tumours also express BDNF, establishing an autocrine pathway which promotes cell growth and survival (119, 120).

Maturing tumours often express the truncated TrkB, whereas most immature, non-amplified tumours express neither (121, 122). The TrkB/BDNF autocrine pathway seems to contribute to both enhanced angiogenesis and to drug resistance (121, 122).

The expression of TrkC is predominantly found in lower stage tumours and, like TrkA and TrkC, is not show in NMYC-amplified tumours (123, 124).

This indicates that favorable neuroblastomas are characterized by the expression of TrkA, with or without TrkC, but unfavorable tumours express full-length TrkB plus its ligand BDNF.

2.5 WNT SIGNALING AND B-CATENIN ACCUMULATION IN NEUROBLASTOMA CELLS

Wnt proteins are a large family (19 in mammals) of glycosylated growth factors that are secreted in a regulated manner from source cells (125). They act as morphogens over short distances to stimulate signaling in responding cells upon receptor binding (126). Wnt signaling is essential for multiple developmental and homeostatic processes, and deregulated pathway activity is associated with multiple disease states (127).

How cells respond to incoming Wnt signals depends on the particular ligand/receptor complex involved, as well as on the cellular context (128). The main classes of Wnt receptors are: the Frizzled proteins (129) and the low-density lipoprotein receptor-related proteins 5 and 6 (LRP5 and LRP6) (130-132).

Wnt signaling is generally subdivided into two pathway classes, being either β-catenin dependent (canonical) or β-catenin independent (non-canonical, such as planar cell polarity) (133, 134).

Frizzled receptors activate both β-catenin-dependent and -independent pathways, whereas LRP5/6 promote more specifically the Wnt/β-catenin pathway (135).

In the Wnt pathway, β-catenin functions as a transcriptional co-activator of Wnt target genes in cooperation with members of the TCF/LEF transcription factors (136). It is also a component of cadherin- cell–cell adhesion complexes at the cell membrane. Whereas β-catenin in adhesion complexes is thought to be relatively stable, the cytoplasmic pool is rapidly degraded by the β-catenin destruction complex, a central player in Wnt signal transduction (137).

In this complex, Axin and adenomatous polyposis coli (APC) promote phosphorylation of β-catenin by casein kinase 1a (CK1a) and glycogen synthase kinase 3(GSK3), resulting in its ubiquitylation-mediated degradation in the proteasome (138-141).

Wnt binding to Frizzled and LRP5/6 leads to inactivation of the destruction complex, allowing β-catenin to accumulate, enter the nucleus and activate target genes (136).

Three events are generally regarded as essential (Fig.2):

1. phosphorylation of LRP6
2. phosphorylation and membrane localization of dishevelled (Dvl) (142), probably by means of Frizzled (143,144)
3. Axin recruitment to phosphorylated LRP5/6 (145)

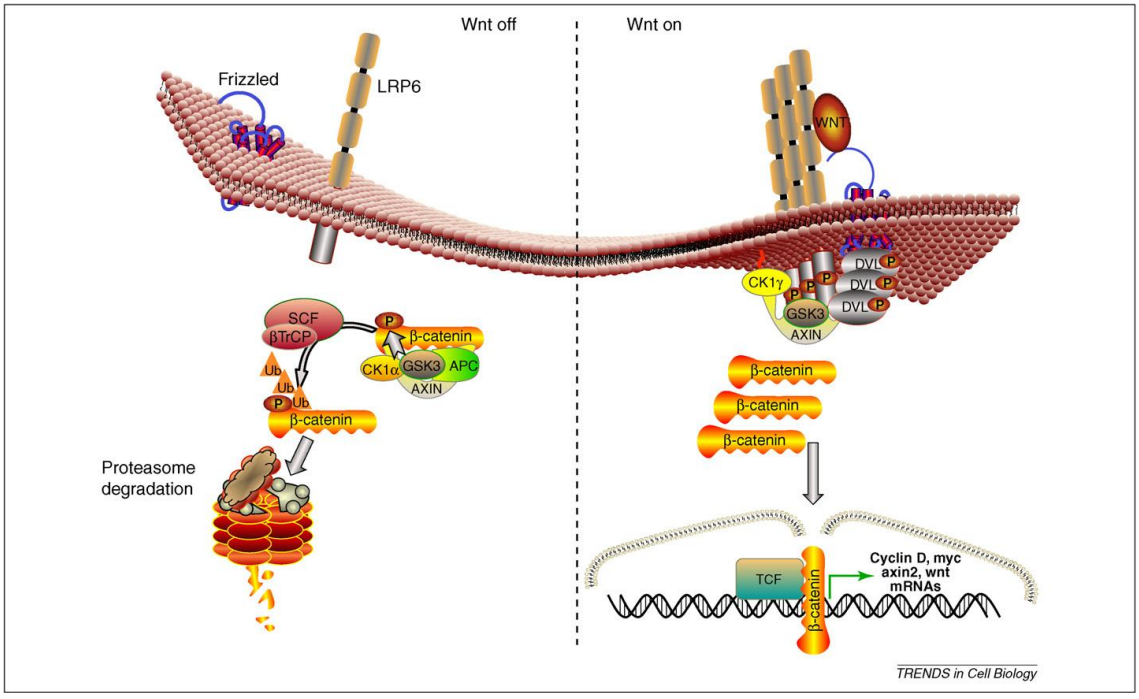

Figure 2: General overview of Wnt/b-catenin signaling.

Wnt-signaling pathway plays an important role in the neuronal development process in vertebrates. In the canonical Wnt/ß-catenin cascade, ß-catenin acts as a central molecule that activates transcription of downstream growth-promoting genes.

ß-catenin is expressed constitutively in neurons and neuroblastoma (146). Many of evidences suggest that the up-regulation of Wnt-signaling pathway has a potential effect on the differentiation status of neuroblasts.

In mouse neuroblastoma cells treated by lithium chloride, inhibition of GSK-3ß by the chemical compound leads to an accumulation of ß-catenin and morphological differentiation (147).

A recent study demonstrates that ß-catenin plays a role in promoting neuronal differentiation of murine neural stem cells (148).

In NB-1 neuroblastoma cell line with MYCN amplification and homozygous deletion of chromosome 1p (149), it is demonstrated that accumulation of ß-catenin in a neuroblastoma cells led to growth inhibition and neurite extension which is related to up-regulation of TrkA. The data suggest a possible availability of ß-catenin as a molecular target for manipulation in the management of neuroblastoma.

The situation is contrasting because, on the other hand, some studies demonstrate that the accumulation of β-catenin is able to inhibit neuronal differentiation by potentiating the NOTCH-RBP-Jκ signaling pathway (150) and also inhibits neuronal differentiation of embryonic stem cells (151).

CHAPTER III

AIM OF THE THESIS

This research project was devoted to amplify the knowledge of sialidase involvement in human tumor pathology. In literature, it is shown that abnormalities in the glycosylation processes are a common marker of cancer; in particular, it has been found an increase of sialic acid content in glycoproteins and an abnormal sialylation in membrane glycolipids (38).

These anomalies lead to the appearance of specific glycosphingolipids that are often absent in healthy cells. These molecules, especially gangliosides, are discharged into the surrounding microenvironment in higher volumes than healthy tissue.

Cancer gangliosides, present on the cell membrane or secreted, appear to play a key role in the progression of the disease since (68) they heavily regulate the adhesion/motility of the cell, participating in the metastatic process. Even in the carbohydrate portion of glycoproteins changes attributable to neoplastic transformation are found and, in particular, is often reported an increase of the sialic acid content. Such abnormalities of membrane glycoproteins, such as selectins and integrins, are functionally important for the cell and are reflected in the adhesion properties and motility of cancer cells, with consequences on the growth and metastatic potential of tumor (64).

These observations justify the interest for many years directed to the study of enzymes that regulate cellular sialic acid content: the sialyltransferases and sialidases.

Scarce evidences are still obtained on the sialyltransferases and on their involvement in neoplastic transformation; in the case of sialidases there are several lines of evidence that suggest their active participation in determining the malignant phenotype. In confirmation, different types of cancer show levels of expression of the four sialidases. In particular, Neu1 down-regulation (69), the disappearance of cytosolic sialidase Neu2 (68) and the over-expression of membrane sialidase Neu3 are frequent in cancer (76). Several indications have shown the involvement of Neu3 in the mechanisms leading to resistance to apoptosis (76). Instead, the inhibition of Neu2 seems to enhance the invasive properties of solid tumors (68) and to reinforce the action of the anti-apoptotic fusion protein Bcr-Abl in chronic myeloid leukemia (73) and Neu1 down-regulation was found to be inversely correlated with metastatic potential (69).

The study of the roles played by Neu4 in cancer is still in a preliminary stage.

The main aim of this research project was to increase the knowledge regarding the sialidases in neuroblastoma. In particular, attention has been devoted to the study of the

last sialidase discovered, therefore, not at all characterized, Neu4. As cellular model, a line of human neuroblastoma, SK-N-BE was used. SK-N-BE cells carry the MYCN oncogene amplification and characteristically express an unusual high level of NEU4L.
In order to clarify the significance of this peculiarity which significantly mark SK-N-BE cells from other NB cell lines classified as low risk, we decided to over-express Neu4L in SK-N-BE cells and study the subsequent effects.
The thesis was planned to develop the following points:

1. Stable Transfection of Neu4L in SK-N-BE cells
2. Assessment of stable transfection
3. Effects on the proliferative potential, cell cycle and differentiation
4. Evaluation of the changes induced by over-expression of the sialidase Neu4L on the signaling pathways
5. Characterization of gangliosides and sialoglycoproteins in order to identify possible candidate molecules substrate of Neu4L action

CHAPTER IV

MATERIALS AND METHODS

4.1 CELL CULTURE

The human neuroblastoma cell lines, SK-N-BE and SH-5Y-SY, were grown at 37°C with 5% CO_2, in RPMI 1640 medium supplemented with 10% (v/v) FBS, 2mM glutamine.

The cryopreservation of these cells is commonly performed in liquid nitrogen and involves the use of freezing medium, contained a mixture of 90% FBS and 10% DMSO.

4.2 STABLE TRANSFECTION OF NEU4L IN SK-N-BE NE CELLS

To perform a stable transfection, we used the plasmid pcDNA3.1/myc-His long 5,493kb.

It contains the following functional elements (Fig.3):

1. PUC ori ensures high replication of the vector in E.coli
2. SV40 early promoter provides an efficient and high expression of the geneticin resistance gene
3. The gene for geneticin resistance allows to select the mammalian cells in which the plasmid is present
4. SV40 pA guarantees the entire transcription and the polyadenylation of the gene for the geneticin resistance
5. PCMV, cytomegalovirus promoter sequence, ensures a high level of expression of the recombinant protein
6. BGH pA guarantees the efficient termination and the polyadenylation of mRNA
7. C-terminal polyhistidine sequence allows the purification of the recombinant protein on metal chelating resins
8. C-terminal Myc Epitope
9. The ampicillin resistance gene allows selection in E. coli
10. The "Multiple cloning site" allows the insertion of the gene of interest and facilitates cloning in frame with the Myc Epitope and the C-terminal polyhistidine sequence.

The cDNA of Neu4L was included in the vector by cutting with the restriction enzymes EcoRI and XbaI.

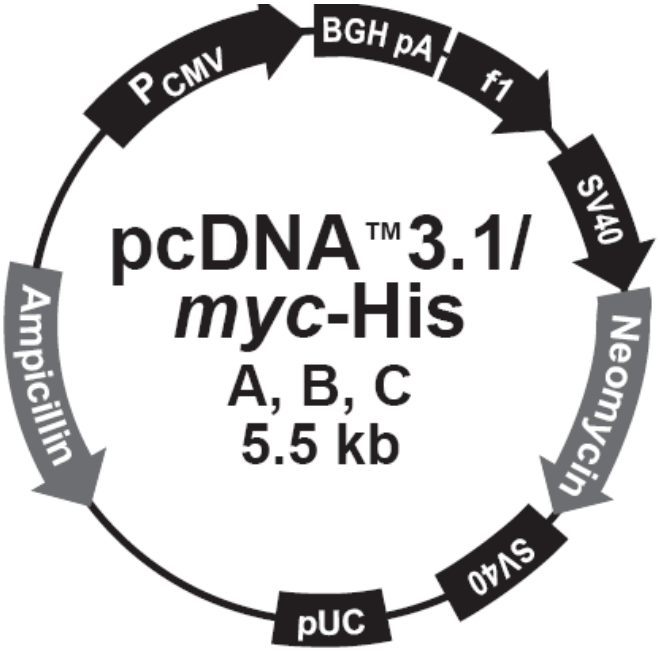

Figure 3: Map of vector pcDNA 3.1/myc-His

4.2.2 BACTERIAL TRANSFORMATION

DH5α E.coli cells, rendered competent by incubation with $CaCl_2$, were incubated on ice for 30 min and then at 42 ° C for 30 sec (thermal shock) with the plasmid pcDNA3.1-MycHis-Neu4L (100ng). The LB medium (1% tryptone, 0.5% yeast extract, 1% NaCl) was added to the cells and the mixture was incubated for 1h at 37 °C while stirring. After incubation the bacteria were resuspended in 100 ml of LB medium with 50 μg/ml ampicillin and cultured at 37 °C overnight.

The GenElute Miniprep Plasmid Kit (Sigma) was used to isolate plasmid DNA from recombinant E.coli cultures. All buffers used for the extraction of the plasmid were included in the Kit and the protocol enclosed was followed.

4.2.2 TRANSFECTION OF pcDNA 3.1 myc/His IN SK-N-BE CELLS

24 hours before transfection, $8x10^5$ cells were plated in 100mm plates in 8 ml of RMPI 1640 medium without antibiotics.

For transfection, two mixtures were prepared:

1. 500 μl of Opti-MEM medium with 8μg DNA
2. 500μl of Opti-MEM medium with 15μl of Lipofectamine 2,000

After leaving the mixture stand for 5 min, the two solutions were combined and incubated for 20 min at room temperature to allow the formation of the complex Lipofectamine 2,000/DNA.
After incubation, the mixture was added to the plate containing the cells.
The cells were then incubated at 37 °C in 5% CO_2 for 4 hours to allow the process of transfection, after, the medium was replaced.

4.3 PROLIFERATION ASSAYS

4.3.1 [^{3}H] THYMIDINE INCORPORATION

24 hours before the assay, $8.5x10^4$ mock and Neu4L over-expressing cells were resuspended in RPMI 1640 contained 10% FBS, 2mM glutamine, 200µg/ml geneticin. Then 0,5µCi/ml [^{3}H]thymidine was added to each well, and after 24 hours at 37°C, the radioactivity incorporated was determined in trichloroacetic insoluble material using a β-Counter.

4.3.2 GROWTH CURVE

$8x10^4$ mock and Neu4L over-expressing cells were seeded in 24-well culture plates, and viable cells were counted every 24 hours with Trypan Blue up to 4 days.

4.3.3 MTT ASSAY

The day before, $2x10^3$ mock and Neu4L over-expressing cells were seeded in 24-well culture plates. MTT was added to the cell in an amount equal to 10% of the culture medium volume. The culture was incubated for 4 hours, at 37°C, 5% CO_2.
After the incubation period, the cells were removed from the incubator and the resulting formazan crystal was dissolved by adding an amount of MTT Solubilization Solution (10% TritonX-100, 0.1 N HCl in anhydrous, 8% isopropanol) equal to the original culture medium volume.
Absorbance was determined by VICTOR spectrophoto/fluorometer at 650 nm to remove the background absorbance and at 570 nm.

4.3.4 SOFT AGAR ASSAY

Concerning the soft agar colony formation assay, 0.72% bactoagar was melt in 1 ml of RPMI 1640 plus 10% FBS and 2mM glutamine to constitute the hard agar layer and was spread into 35-mm dishes.

$1.5x10^4$ cells were rapidly suspended in 1 ml of RPMI 1640 containing 10% FBS, 2mM glutamine, and 0.36% bactoagar, at 37 °C, and were distributed onto the hard agar layer. Then the plates were incubated at 37 °C for 2 weeks, and the cell colonies were counted.

4.4 INDUCTION OF DIFFERENTIATION

Mock and Neu4L over-expressing cells were grown in line at 37 ° C with 5% CO_2 for 6 days in RPMI 1640 medium supplemented by 1% (v/v) FBS, 2mM glutamine, 200μg/ml geneticin.

The cells were harvested at different times: 1 day, 2 day, 3 day and 6 day. After 6 days the medium was replaced with one containing 10% FBS, and cells were harvested at different times: 1^{st} day and 2^{nd} day.

4.5 RNA EXTRACTION

The total RNA was isolated from SK-N-BE cells using the RNeasy mini Kit (QUIAGEN), which includes columns with silica membranes for the purification of RNA and appropriate buffers.

$8x10^5$ cells were plated, detached from culture plate with trypsin, and pelleted at 300xg, 5 min at 20 ° C

Subsequently the samples were homogenized and lysed by adding of lysis buffer.

RNA was extracted following the manufacturer's instructions and was collected in 40μl of water. The 800ng of total RNA was reverse-transcribed employing the iScript cDNA Synthesis Kit (Bio-Rad Laboratories)

4.6 RNA ASSAY

The RNA assay was performed using RiboGreen, a reagent containing cyanine.
RiboGreen has a maximum of excitation at 500 nm and an emission maximum at about 525 nm.
An aqueous RiboGreen mixture was prepared, diluting the stock solution 1:200 with TE buffer (10 mM Tris/1 mM HCl, EDTA, pH 7.5), and a calibration curve using a mixture of rRNA (16S and 23S) was set up.
100μl of aqueous RiboGreen solution was added to each sample. Therefore, the fluorescence was measured on samples and standards.

4.7 RETRO-TRASCRIPTION

RNA was reverse transcribed by using of the iSCRIPT cDNA Synthesis Kit (Biorad) which consists of the following reagents:

1. 5x iScript Reaction Mix, a mixture that includes random hexamers, oligo-dT, RNase inhibitor, dNTPs.
2. Nuclease-free water, used to bring to volume the mixture.
3. IScript Reverse Transcriptase

4μl of Reaction Mix, 1μl Reverse Transcriptase, and nuclease-free water to final volume of 20μl were added to 800ng of RNA
The mixture was incubated for:

1. 5 min at 25 ° C
2. 30 min at 42 ° C
3. 5 min at 85 ° C

A negative mock containing only RNA and water was prepared to verify the absence of genomic DNA contamination.

4.8 POLIMERASE CHAIN REACTION (PCR)

The reaction mixture was as follows:

- cDNA
- Buffer (20 mM Tris-HCl, 50 mM KCl, pH 8.4)
- 1.5 mM $MgCl_2$
- 200 nM dNTPs mix
- 200 nM Forward primer
- 200 nM Reverse primer
- (2U) Taq-DNA polymerase

Amplification was achieved using an Eppendorf thermal cycler, following the protocol described here:

1. denaturation: 95 °C, 2 min

2. denaturation: 94 °C, 30 sec
3. annealing: 58 °C, 30 sec
4. elongation: 72 °C, 30 sec

} repeated 37 times

5. elongation: 72 °C, 4 min

Gene	Forward	Reverse
NEU4L	TGAGCTCTGCAGCCTTCC	GTTCATGGACCGGTGCTC

Table n°1: Primers used for PCR

4.9 REAL-TIME PCR

The reaction mixture, prepared in a final volume of 20 µl, contained:

- cDNA: 30 ng
- 200 nM Primers:
- 21µl of SYBR Green Super Mix (Biorad)

Moreover, a black without cDNA was prepared for each simple to check the possible contaminations

iCycler Bio Rad thermocycler was used, following this program of amplification:

denaturation: 95°C, 2 min

denaturation: 95°C, 15 sec
annealing:
elongation: 58°C, 30 sec
detection of:
fluorescence:

} repeated 40 times

At the end of amplification cycles "melting curve" was performed to exclude the presence of non-specific products.

The results were processed using the software equipment available

Gene	Forward	Reverse
ACTβ Sh	CGACAGGATGCAGAAGGAG	ACATCTGCTGGAAGGTGGA
NEU4L	CTCTGCAGCCTTCCCAAG	GTCCTCTCCCGCTCGAAG
NMYC	CCCTACGTGGAGAGTGAGGA	GTGAGAAAGCTGGACCGAAG
MYC	ACGTCTCCACACATCAGCAC	CGCCTCTTGACATTCTCCTC
P27	CTCGAGGACACGCATTTGG	CACGAACCGGCATTTGG
P21	TGCCCAAGCTCTACCTTCC	ACAGGTCCACATGGTCTTCC
CYCLIN D2	TTACCTGGACCGTTTCTTGG	CCTGAGGCTTGATGGAGTTG
AXIN2	GGCTCCAGAAGATCACAAAG	TATGGAATTTCCTTCCCCACA
DSH1	GACATCACTTTCTGGCATC	TCGTCATTGCTCATGTTCTC
GSK3β	ATGTATGGTCTGCTGGCTGT	TTCTCTGATTTGCTCCCTTG
βCATENIN	AGCTCTTACACCACCATCC	GCACGAACAAGCAACTGAAC
NESTIN R	CCAAGAACTGGCTCAGGAAA	TCTCCCTGCTCTACCACCTC
CD133	CTAGCCTGCGGTCATCTCTC	AGGCCATCCAAATCTGTCCT
OCT4	AGGAGAAGCTGGAGCAAAA	GGCTGAATACCTTCCCAAA
NANOG	GGTCCCAGTCAAGAAACAGA	GAGGTTCAGGATGTTGGAGA

Table°2: Primers used for REAL-TIME PCR

4.10 PROTEIN ASSAYS

Two methods were used for protein assay: Bradford's and Lowry's methods.

4.10.1 BRADFORD ASSAY

A standard calibration curve with BSA (bovine serum albumin), at known concentrations, was prepared to determine the protein concentration of the samples.
1 ml of blue dye Coomassie diluted in water 1:4 was added to each samples; then, absorbance was detected with a JASCO spectrophotometer, at 595 nm.

4.10.2 LOWRY ASSAY

1ml of the following solution is added to the samples and to the standards prepared with BSA at known concentration:

- 2% Na_2Co_3 in 0.1N NaOH
- 1% $CuSO_4$
- 2% $C_4H_4KNaO_6*4H_2O$

The mixture was incubated for 10 min at room temperature; then, 100µl of the Folin Ciocalteu reagent, diluted 1:1, in water were added.
The samples were incubated for 30 min, at room temperature. The detection was performed at 750 nm, with a spectrophotometer JASCO.

4.11 SIALIDASE ACTIVITY ASSAY

Mock and Neu4L over-expressing cells were harvested from plates 100 mm, at approximately 80% of confluence, scraping in PBS (8.1 mM Na_2HPO_4, 1.5 mM KH_2PO_4, 2.7 mM KCl, 137 mM NaCl, pH 7.4). The cells were centrifuged at 400xg for 5 min at 4 °C. The supernatant was eliminated and the pellet containing cells was re-suspended in PBS supplemented with protease inhibitors (10µg/ml leupeptin, 10µg/ml aprotinin, 10µg/ml pepstatin). Cells were lysed by sonication (2 cycles of 8 sec, 1 min interval).
The mixture was centrifuged at 800xg for 10 min at 4 °C to remove the unbroken cells and nuclei from "crude homogenate". Subsequently, the crude homogenate was

centrifuged at 70,000xg, for 20 minutes, at 4 °C, to separate the cellular membranes from cytosol.

The pellet, resuspended in PBS, was used for sialidase activity.

The activity was expressed as U/mg protein: 1U equals to 1µmole substrate of released in 1 min.

A fluorimetric, radiochemical and colorimetric assay were performed.

The fluorimetric assay relies on the use of artificial fluorescent substrate methylumberilliferyl-N-acetily-D-neuraminic acid (MU-NeuAc) (152).

The activity was assayed using membrane proteins extracted from cells.

The preparation of the reaction mixture was carried out as follows:

- 50 mM Citrate phosphate buffer, pH 3.2
- 0.1 mM MU-NeuAc
- 600 µg BSA
- 20-25 µg of proteins containing the enzyme

The mixture was brought to a final volume of 100µl with H_2O.

"White" samples were also prepared, containing all components except the enzyme preparation.

The samples were incubated at 37 °C, with shaking, for 1 hour. After incubation, 0.2 M glycine pH 10.8 was added to stop the reaction.

The amount of 4-methylumberilliferyl released by the enzyme was determined by measuring the fluorescence emitted.

The standard samples were prepared with 0.5 nmol of MU-Na, in a final volume of 100µl. The fluorescence was determined using Nanodrop fluorometer (excitation: 365λ emission: 448λ)

The radiochemical method uses GD1a ganglioside, a natural substrate of sialidase radioactively labeled with tritium on the carbon chain of sphingosine (153).

The [^{3}H] GD1a and the residual [^{3}H] GM1, released by the sialidase, were separated by thin layer chromatography (HPTLC) and detected by analysis with radiocromatoscanner Beta-Imager (Biospace).

The ganglioside micelles were prepared by mixing 173,000dpm (equivalent to 0.45 µCi/mole) of [^{3}H] GD1a dissolved in propanol/water 7:3, and 20nmoli of cold GD1a, dissolved in chloroform / methanol 2: 1.

The solvents were evaporated under the nitrogen and the gangliosides were resuspended in 20 µl of water.

The reaction mixtures were prepared in a final volume of 100µl and were composed as follows:

- 20nmoli, 173,000dpm [^{3}H] GD1a micelles
- 50 mM citrate phosphate buffer, pH 3.2
- 20-25 µg of membranes
- 0.04% Triton X-100

"White" samples were prepared, including all reaction components without the enzyme.

The samples were incubated for 1 hour, at 37 °C with shaking.

After incubation, the reaction was stopped by rapid freezing and subsequent addition of 4 volumes of tetrahydrofuran (400µl).

The reaction products were separated by HPTLC on silica plates using as solvent a mixture of chloroform/methanol/0.2% $CaCl_2$ (60:40:9).

Colorimetric method was used to assay sialidase activity towards glycoproteins, as fetuin.

The reaction mixture was prepared in a final volume of 100µl and was composed as follows:

- 100µg Fetuin
- 50 mM citrate phosphate buffer, pH 3.2
- 40µg of membrane proteins

The mixture was incubated for 2 hours at 37°C in shaking; at the end of incubation the reaction was stopped by freezing at -20.

A resin (DOWEX 1x8 200-400 mesh) was used to bind the extracted sialic acid by the previous reaction.

The samples were acidified by adding of 1N H_2SO_4 in a final volume of 100µl; in the same way the standard was made.

The samples were loaded onto the resin, washed 7 times with 1ml of H_2O and were eluted by adding of 2N $C_2H_3NaO_2$ pH 4.6 (about 1,2 ml); then Warren assay was made to measured the free sialic acid.

400µl of periodate reagent (sodium periodate (meta) 0.2M in 9 M H_3PO_4) was added to the assay samples and the tubes were incubated for 20 min at 20°C; then, 1ml of 10%

sodium arsenite (in 0.5 M Na_2SO_4 and 0.1 N H_2SO_4) and 3 ml of 0.6% thiobarbituric acid (in 0.5M Na_2SO_4) were added to the samples and the mixture was incubated for 15 min at 100°C.

Cyclohexanone was added (4 ml) to the samples to extract the colorimetric signal. The solution was centrifuged at 1,000 xg for 10 min and absorbance was detected at 550 and 532 nm.

4.12 ELECTROPHORESIS

4.12.1 NUCLEID ACID ELECTROPHORESIS

Samples were run in a 1% agarose gel, prepared by melting agarose in TAE (0.4 mM Tris/acetate, 10 M EDTA, pH 8.3). 0.5μg/ml ethidium bromide was added to the mixture.

The run was performed in TAE buffer, at a constant voltage of 100V.

Samples were dissolved in a loading buffer consisting of 0.04% Bromophenol blue and 5% glycerol in water.

4.12.2 PROTEIN ELECTROPHORESIS

A discontinuous gel, consisting of a stacking and a running gel, was prepared.

Running Gel Composition (12% -10%: Acrylamide):

- H_2O
- 1.5 M Tris/HCl pH 8.8
- 10-12% Acrylamide
- 0.1% w/v SDS
- 0.05% w/v APS (ammonium persulphate)
- TEMED

Stacking Gel Composition (4% Acrylamide):

- H_2O
- 0.5 M Tris/HCl pH 6.8
- 0.1% w/v SDS
- 4% acrylamide
- 0.05% w/v APS

- TEMED

The cells were harvested and broken by sonication and the lysed cells were centrifuged at 800xg, 10 min at 4 °C to separate unbroken cells and nuclei from the so-called "crude homogenate". Subsequently, the crude homogenate was centrifuged at 70,000xg, for 20 min, at 4 °C, in order to obtain the precipitation of cell membranes. The samples, consisting of 20 μg of crude homogenate or membrane proteins, were diluted in loading buffer (62.5 mM Tris/HCl pH 6.8, 2% SDS, 10% glycerol, 5% 2-mercaptoethanol, 0.01% Bromophenol blue) and were boiled for 3 min.

The electrophoresis was performed in 25 mM Tris/HCl, 19.2 mM glycine, 0.1% SDS, pH 8.3, at constant amperage of 18 mA. After running, proteins were transferred onto PVDF membrane for Western blot.

4.13 WESTERN BLOT

20 μg of proteins were transferred to a PVDF membrane at 100 V, for 2 hours, at 4 ° C. In order to saturate nonspecific binding sites, the membrane was incubated for 1 hour or over-night in a Blocking Buffers of different composition depending on the basis of the primary antibody used: Blocking Buffer consisting of TBS (50 mM Tris/HCl, 0.15 M NaCl, pH 7.5), 0.1% (w/v) Tween 20 with or 1% BSA, used for the characterization of phosphorylated proteins, or 5% non fat milk powder in all other cases.

The membrane was washed in TBS and 0.1% Tween 20 and then, the primary antibodies, appropriately diluted in Blocking Buffer, were added and incubated for 1 hour or over-night.

The following primary antibodies were used:

Antibody	*Source*	*Dilution*
Myc epitope	Mouse	1:400
Cytochrome C	Mouse	1:1,000
β-catenin	Mouse	1:5,000
P-cdk2	Rabbit	1:1,000
Nmyc	Rabbit	1:1,000
v-Src	Rabbit	1:1,000

Cytochrome P450	Rabbit	1:1,000
P-Rb 807/811	Rabbit	1:1,000
NCAM	Rabbit	1:1,000
Lamp2	Goat	1:1,000

Table 3: antibodies used for Western blot

The membrane was washed several times in TBS and 0.1%.Tween 20
Then, the membrane was incubated for 1 hour with the secondary antibody conjugated with peroxidase, diluted 1: 2,000 in Blocking Buffer.
Following the final wash, the detection of the antibody complex was performed with the SuperSignal West Pico/Dura Trial Kit (Pierce).

4.14 SIALOGLYCOPROTEIN ASSAY

30μg of cytosolic and membrane proteins were separated by SDS-PAGE on 10% polyacrylamide gel and then transferred onto PVDF membrane , at 100 V for 2 hours, at 4 °C.
Sialoglycoproteins were visualized using the DIG (Glycan Differentiation Kit-Roche Applied Science) and following manufacturer's protocol. In particular, we used lectin MAA (Maack amurensis agglutinin) to identify glycoproteins containing sialic acid $\alpha 2 \rightarrow 3$ linked to galactose, and the SNA lectin (Sambucus Nigra agglutinin) for the identification of glycoproteins containing sialic $\alpha 2 \rightarrow 6$ acid bound to galactose.
The membranes were incubated overnight with a blocking buffer consisting of TBS BUFFER and 5% milk powder. Then, we proceeded with 2 washes of 10 min in TBS and a further wash of 10 min in buffer 1 (TBS, 1 mM $MgCl_2$, 1 mM $CaCl_2$, pH 7.5).
After washing, the membranes were incubated for 1 hour with the lectin conjugated to digoxigenin.
After incubation, the membranes were washed 3 times, for 10 min, in TBS, and then incubated for 1 hour with an anti-digoxigenin antibody conjugated with alkaline phosphatase.

After 3 additional washes in TBS, antibody complexes were visualized by adding the chromogenic substrate NBT/X-phosphate, dissolved in buffer 2 (0.1 M Tris/HCl, 0.05 M $MgCl_2$, 0.1 M NaCl, pH 9.5).

4.15 LUCIFERASE ASSAY

The day before, $6x10^4$ cells were seeded in 24-well culture plates in 500 µl of RPMI plus 10% FBS and 2mM glutamine.

Cells were transfected with TOPFlash (TCF Reporter Plasmid), vector carrying a promoter responsive to β-catenin upstream the luciferase gene.

In particular it contains 2 sets (with the second set in the reverse orientation) of three copies of the TCF binding site (wild type) upstream of the Thymidine Kinase (TK) minimal promoter and Luciferase open reading frame.

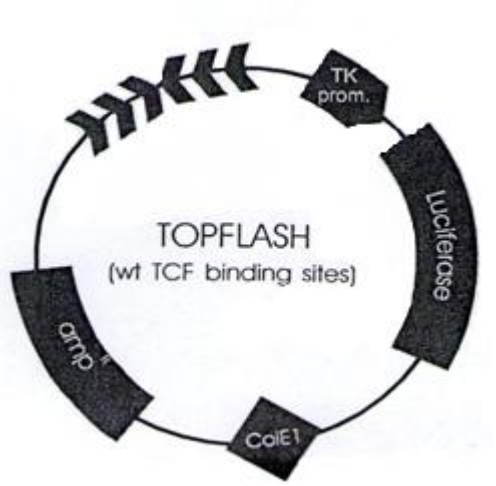

Figure 4: map of vector TOPFLASH

The transfection was made as described below:

1. 750 ng of TOPFlash were diluted in 100 µl Opti-MEM
2. 1µl of PLUS Reagent (Invitrogen) was directly added to the diluted DNA. The solution was mixed and incubated for 5 min
3. 4µl of Mix Lipofectamine LTX (Invitrogen) was added to the mixture and mixed thoroughly.
4. The solution was incubated for 30 min, at room temperature

5 100µl of DNA-lipid complex were added to the cell, and were incubated for 12 hours at 37°C, 5% CO_2

The next day, the medium containing DNA-lipid complex, was removed and replaced with 200µl of RPMI1640 with 10% FBS and 2mM glutamine. The cells were incubated for 24 hours at 37°C, 5% CO_2.

At the end of the incubation, the activation of the reporter assay was followed using the luciferin (Promega). The luminometric signal was measured by a VICTOR luminometer (Wallac).

4.16 METABOLIG LABELING OF CELL SPHINGOLIPIDS WITH [3-^{3}H] SPHINGOSINE

The sphingolipid pattern of SK-N-BE cells was determined by metabolic labeling with [3-^{3}H] sphingosine ([3-^{3}H] SPH). [3-^{3}H] SPH is a natural precursor of sphingolipids.

When cells are placed in culture medium supplemented with radiolabeled sphingosine, [3-^{3}H] SPH is absorbed and used into the biosynthetic pathways of sphingolipids. The metabolic products are radioactive, and after extraction and separation by HPTLC, it is possible to evaluate the cellular sphingolipid content in terms of both quality and quantity.

(0.4 µCi) [3-^{3}H] SPH was administered to the cells after being dissolved in culture medium at a final concentration of $3x10^{-8}$M. Subsequently, the lipids were extracted and separated by HPTLC and the chromatographic profile was read by Beta-Imager equipment (Biospace).

1. *DISSOLVING OF SPHINGOSINE*:

   [3-^{3}H] SPH was dissolved in sterile conditions in RPMI 1640 medium with 10% FBS, 2 mM Glutamine.

   The solution was sonicated for 2 min and vortexed for 1 min. This procedure was repeated 3 times. The degree of solubilization (> 70%) was verified by counting the radioactivity by β-counter (Perkin Elmer).

2. *PULSE:*

The day before, $8x10^5$ cells were plated.

The culture medium was replaced with 5ml of medium containing [3-^{3}H] SPH.

The cells were then incubated for 2 hours at 37 °C, with 5% CO_2.

In this phase the cells absorbed the [3-^{3}H] SPH present in the medium.

After two hours, the medium was taken from plates and stored for the quantification of [3-^{3}H] SPH absorbed by cells, by counting the radioactivity with a β-counter (Perkin Elmer).

3. *CHASE*

The cells were grown in 8ml of growth medium without [3-^{3}H] SPH, for 24 hours, at 37 ° C with 5% CO_2.

4. *CELL HARVESTING*

At the end of the chase, medium was collected from plates and kept for counting by β-Counter (Perkin Elmer). The cells were washed three times with PBS and harvested.

After being harvested by centrifugation (300xg, 10 min, 4 °C), the cells were freeze and lyophilized

5. *EXTRACTION OF TOTAL LIPIDS FROM CELL PELLET*

The lyophilized cells were resuspended in 25µl of water, sonicated in ultrasonic bath and vortexed. In order to obtain a good solubilization, two lipid extractions were made.

<u>FIRST EXTRACTION</u>

10 volumes of methanol were added to the aqueous solution of cells. The resulting mixture was sonicated in ultrasonic bath for 2 min and vortexed for 1 min.

Then, 20 volumes of chloroform were added. Sonication in ultrasonic bath for 2 minutes and agitation were repeated.

The samples were shaken on an Eppendorf shaker for 10 min and centrifuged at 10,000xg, for 10 min at room temperature.

The supernatant containing the lipids was transferred to a new eppendorf.

SECOND EXTRACTION

10 volumes of a mixture of chloroform / methanol 2:1were added to pellet.

The samples were sonicated in ultrasonic bath, vortexed and shaken for 10 min; then, they were centrifuged at 10,000xg, for 10 min, at room temperature. The lipid supernatant was collected and combined with that collected after the first extraction.

The protein pellets, after the evaporation of solvent, was digested overnight at room temperature in 50µl of 1N NaOH and then, subsequently, increased to 1 ml with water.

Proteins were then measured by the method of Lowry.

The lipid radioactivity was evaluated to determine the percentage yield of the lipid extraction.

PARTITION OF LIPIDS

This procedure allows to divide the extracted lipid in an aqueous phase (FA), containing gangliosides, and an organic phase (FO), containing neutral glycolipids.

The partition was divided into two phases:

FIRST PARTITION

In order to separate the aqueous from the organic phase, a volume of water equal to 20% of the total solution was added to lipid extracts. Samples were vortexed and mixed on Eppendorf mixer for 15 min and centrifuged at 3,500xg for 5 min. The aqueous phase was collected and transferred to a new eppendorf.

SECOND PARTITION

A mixture of methanol / water 1: 1, equal to 40% of the initial volume, was added to the organic phase. The separation of the aqueous phase from the organic phase was obtained by vortexing and agitation on an Eppendorf shaker for 15 min and, finally, centrifugation at 3,500xg for 5 min.

The aqueous phase was collected and added to that obtained in the first separation.

The two separated phases were dried under nitrogen and suspended in a mixture of chloroform/methanol 2:1. The aqueous phase was resuspended in 100 µl of solvent, while the organic phase was resuspended in 200 µl.

Radioactivity assays of the two phases were performed to determine the percentage yield of the partition. The total lipids, neutral glycolipids and gangliosides were then separated by HPTLC and the content of the component detected was expressed as dpm / mg total protein.

In order to separate total lipids and gangliosides was used a solvent consisting of chloroform/methanol/0.2% $CaCl_2$ (60:40:9) and to separate neutral lipids in the organic phase, a solvent consisting chloroform/methanol/water (110:40:6).

4.17 FLOW CYTOFLUORIMETRY

Cells were labeled with 20 µM BrdU for 15 min at 37°C harvested, and fixed in 70% ethanol. Fixed cells were incubated in 3N HCl for 15 min, washed with 0.1 M $Na_2B_4O_7$, pH 8.5, and finally stained sequentially with monoclonal anti-BrdU (BD Biosciences) in PBS, 0.5% Tween 20, 1% BSA, and anti-mouse Alexa488 antibody (Invitrogen Life Technology). Later, the cells were resuspended in PBS containing 3 µg/ml propidium iodide RNase and 1%BSA, and stained overnight at 4°C in the dark. Cell analysis was performed on at least 30,000 events for each sample by FACSCalibur System (BD Biosciences) and the DNA profile was analyzed by Summit 4.3 (Cytomation Coulter, Glostrup, Denmark).

4.18 CELL SUBFRACTIONATION

In order to obtain mitochondria, lysosomes, reticulum endoplasmatic, membrane and cytosol, $2x10^7$ Neu4L over-expressing cells were plated, harvested and sub-fractionated as fellow.

4.18.1 MITOCHONDRIA ISOLATION

We used the mitochondria isolation Kit (PIERCE) to isolate mitochondria.

$2x10^7$ cells were harvested and centrifuged at 850xg for 2 min; then we followed the manufacturer's instructions.

4.18.2 LYSOSOME ISOLATION

The lysosomes were obtained from the supernatant previously obtained after mitochondria isolation; in particular, it was centrifuged at 12,000xg for 15 min at 4°C. This supernatant fraction (PMF), which is post mitochondria fraction, is the source of microsomes while the pellet contains the lysosomes.

4.18.3 ENDOPLASMATIC RETICULUM ISOLATION

In order to separate endoplasmatic reticulum, we used Endoplasmatic Reticulum isolation Kit (SIGMA). The PMF was transferred to a beaker containing a suitable magnetic spinbar and a volume of 8mM Ca_2Cl, equivalent of 7,5 times the volume of PMF, was added to the PMF with constant stirring. After, the mixture stirred for additional 15 min. The sample was centrifuged at 8,000xg for 10 min at 4°C. The obtained pellet contained the enriched RER microsomes

4.18.4 MEMBRANE AND CYTOSOL ISOLATION

The supernatant, isolated after RER preparation, was centrifuged at 70,000xg for 20 min at 4°C.

The pellet contained cell membranes while the supernatant was the cytosol.

CHAPTER V

RESULTS

5.1 SIALIDASE NEU4 GENE EXPRESSION IN NEUROBLASTOMA CELL LINES SH-SY5Y AND SK-N-BE

Total RNA was extracted to determine the sialidase Neu4 gene expression in SK-N-BE and SH-SY5Y cells, as described in materials and methods.

The RNA was reverse transcribed and the cDNA was analyzed by Real Time PCR.

Then, the values were normalized to the housekeeping gene encoding β-actin.

Neu4 expression was quantitatively assessed and compared in two different neuroblastoma cell lines, SK-N-BE and SH-SY5Y cells. SK-N-BE cells showed a 3.57-fold increase of Neu4 mRNA in comparison to SH-SY5Y (Fig. 5.1).

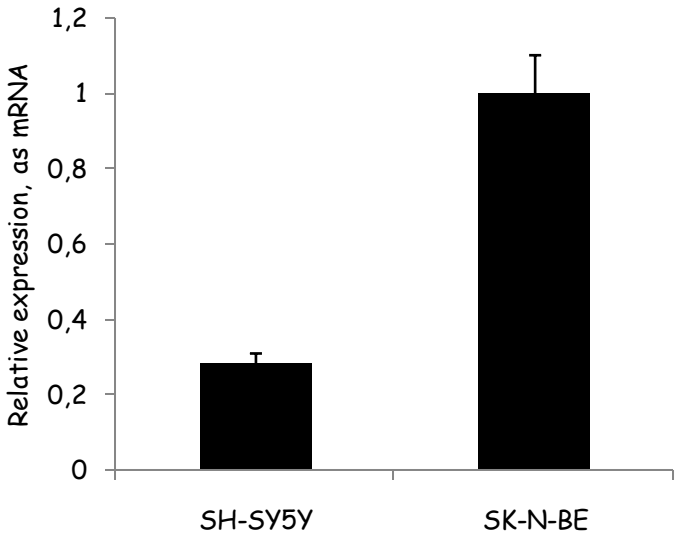

Figure 5.1: Neu4 expression in SH-SY5Y and SK-N-BE cell lines

5.2 OVER-EXPRESSION OF SIALIDASE NEU4L IN SK-N-BE CELLS

SK-N-BE cells were transfected with the recombinant vector pcDNA 3.1-myc-His-Neu4L, using the procedure described in materials and methods.

Selection in 200 μg/ml geneticin began 48hours after transfection and after 2 weeks individual colonies were isolated using cloning disks.

In order to assess the efficiency of the stable transfection, two different approaches were adopted:

- Determination of Neu4L mRNA increase by Real Time PCR
- Determination of sialidase activity in the particulate fraction, at pH 3.2

5.2.1 SIALIDASE NEU4L GENE EXPRESSION IN SK-N-BE TRANSFECTED CELLS

After selection, 3 different clones were isolated and compared to mock cells.

Total RNA was extracted and reverse transcribed from these clones, as described in materials and methods, to verify the presence and the increase of NEU4L expression.

Neu4L over-expression was evaluated by REAL-TIME PCR (Fig. 5.2).

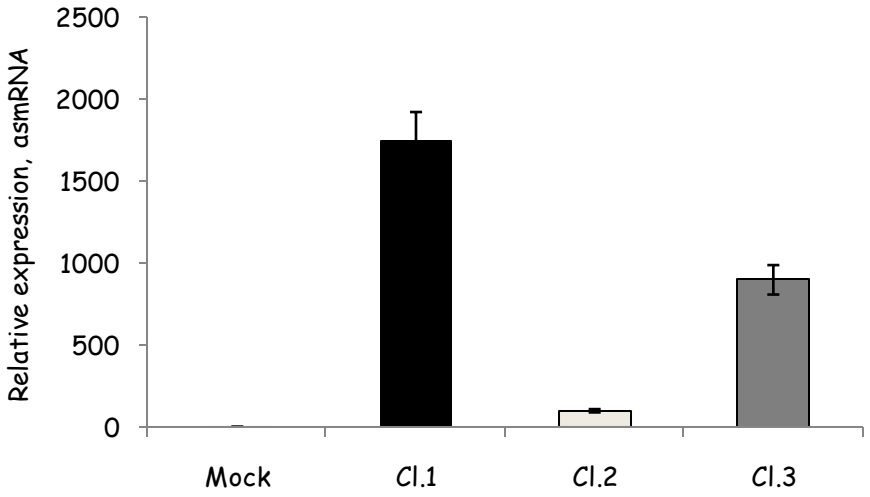

Figure 5.2: Neu4L expression in mock and over-expressing cells

Neu4L over-expressing cells showed a net increase of NEU4L expression, in comparison to mock cells. Among the selected clones, Neu4L Cl.1 exhibited a 1,700-fold increase of NEU4L expression in comparison to mock cells. We decided to continue the experiments on this clone.

5.2.2 SIALIDASE ACTIVITY ON CELL MEMBRANES OF NEU4L OVER-EXPRESSING CELLS

The cell membranes of mock and Neu4L over-expressing cells were obtained using the protocol described in materials and methods. The sialidase activity was subsequently assayed at pH 3.2 toward the artificial substrate methylumberilliferyl-N-acetily-D-neuraminic acid (MU-NeuAc).

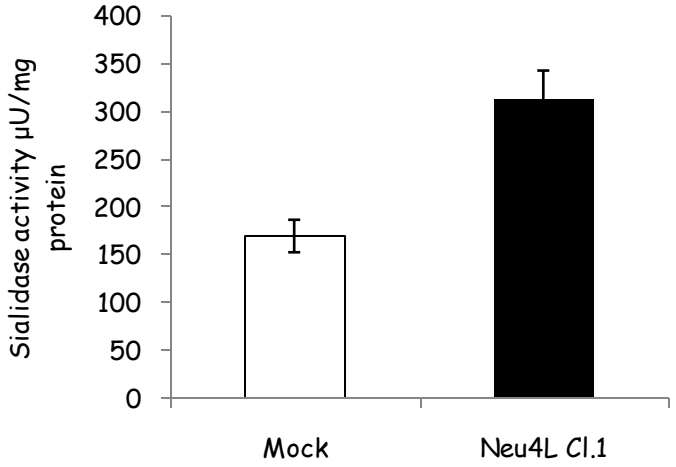

Figure 5.3: sialidase activity towards MU-NeuAc at pH 3.2

The sialidase activity was estimated equal to 312 µU/mg in Neu4L over-expressing cells, while in mock cell it was 170 µU/mg. Therefore, we assessed a 1.83-fold increase of sialidase activity in Neu4L over-expressing cells in comparison to mock cells (Fig 5.3).

Moreover, we assayed sialidase activity towards fetuin, as a representative sialoglycoprotein, at pH 3.2 (Fig 5.4); we also decided to evaluate the activity at pH 7 to demonstrate that the sialidase worked at physiological pH.

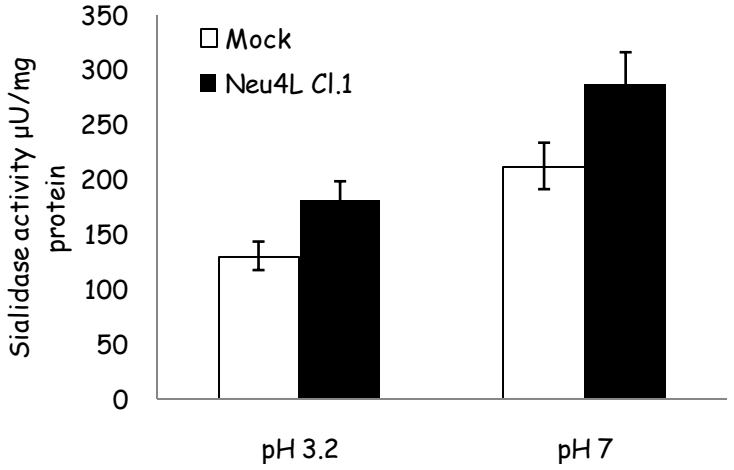

Figure 5.4: sialidase activity towards Fetuin at pH 3.2 and pH 7

Neu4L over-expressing cells showed a sialidase activity equal to 180 µU/mg, while mock cells equal to 130 µU/mg; there was a 1.4-fold increase in Neu4L over-expressing cells at pH 3.2.

We found the same increase at pH 7; in fact, Neu4L over-expressing cells showed an activity value equal to 287µU/mg vs 212µU/mg in mock cells.

These results demonstrated that cells, transfected with pcDNA3.1 Myc/His- Neu4L, stably over-expressed the sialidase Neu4L and that the enzyme was also active at physiological pH towards sialoglycoproteins.

Cell membranes were also used to determinate the sialidase activity towards ganglioside GD1a, as described in materials and methods, but we did not find differences between mock and Neu4L over-expressing cells.

5.3 SIALIDASES NEU1 AND NEU3 GENE EXPRESSION

In order to make sure that the transfection with Neu4L did not alter other sialidases behaviour, we evaluated sialidase NEU1 and NEU3 gene expression by Real Time PCR.

Sialidase NEU2 is not expressed by SK-N-BE cells.

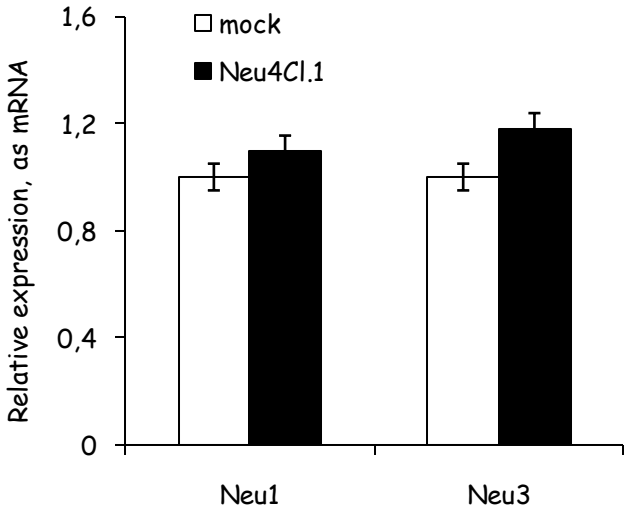

Figure 5.5 Gene expression of sialidases NEU1 and NEU3

Sialidases NEU1 and NEU3 did not show significant alterations in gene expression between mock and Neu4L Cl.1 cells (Fig 5.5).

5.4 NEU4L LOCALIZATION

Mitochondria, endoplasmatic reticulum, lysosomes, membrane and cytosol were obtained as described in material and method.

The proteins were separated by SDS-PAGE and transferred to PVDF membrane.

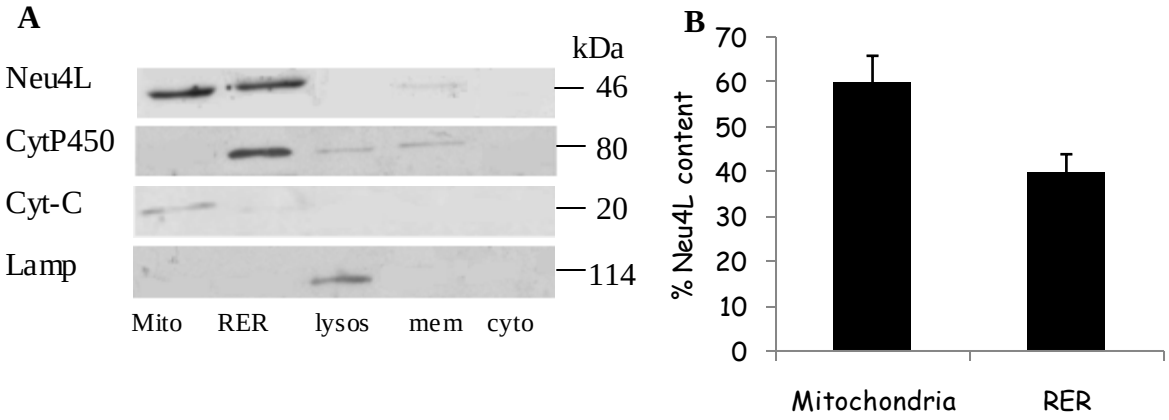

Figure 5.6: Characterization of Neu4L localization: A) Western Blot, B) densitometric analysis

Neu4L seemed to be localized in mitochondria and RER, while it was not present in lysosomes, membrane and cytosol. The efficiency of sub-fractionation was followed by the analysis of specific markers. The localization of Neu4L was identified to be in mitochondria (60%) and in RER (40%) (Fig. 5.6).

5.5 EFFECTS OF NEU4L OVER-EXPRESSION ON SK-N-BE MORPHOLOGY

As showed in Fig 5.7, mock cells seemed to be smaller and with a well-defined cell body; Neu4L over-expressing cells seemed to be larger than mock cells and more adhesive to the plate. Therefore, Neu4L over-expression induced some significant morphological changes.

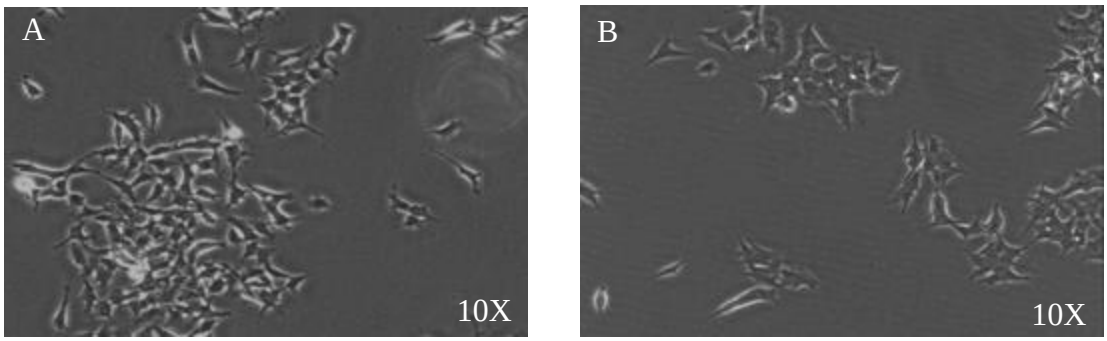

Figure 5.7: Phase contrast microphotographas of A) mock cells B) Neu4L over-expressing cells

5.6 EFFECTS OF NEU4L OVER-EXPRESSION ON THE PROLIFERATION RATE OF SK-N-BE CELLS

We carried out several experiments to evaluate the proliferative potential of transfected cells:

- Growth Curve
- [^{3}H]Thymidine incorporation
- MTT assay
- Soft Agar Assay

5.6.1 GROWTH CURVE

Mock and Neu4L over-expressing cells were plated and counted after staining with Trypan Blue, at intervals of 24 hours, up to 4 consecutive days, as described in materials and methods. It was possible to create a growth curve to compare the proliferative potential of mock and Neu4L Cl.1 cells.

As shown in fig. 5.8, it was clear that the over-expression of Neu4L caused a marked increase of proliferation rate in comparison to mock cells. At 4th day of cell culture, Neu4L over-expressing cells showed 1.56-fold increase in comparison to mock cells.

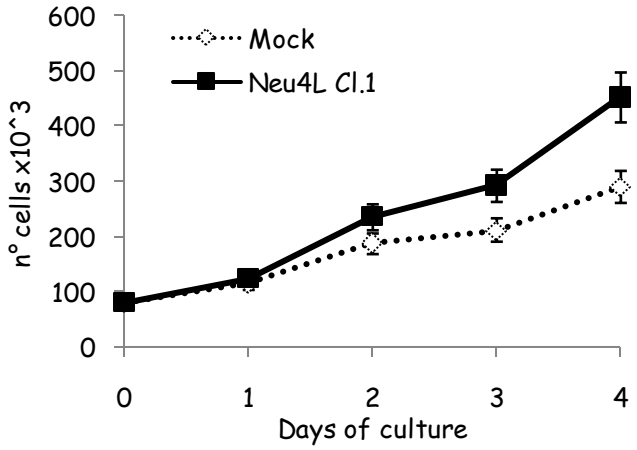

Figure 5.8: Growth curve

5.6.2 [^{3}H] THYMIDINE INCORPORATION

In order to confirm the increase of the proliferation, identified by growth curve, we decided to determinate the capacity to incorporate [^{3}H] thymidine.

Neu4L over-expressing cells showed a 1.58-fold increase of [^{3}H]thymidine incorporation in comparison to mock cells (Fig.5.9).

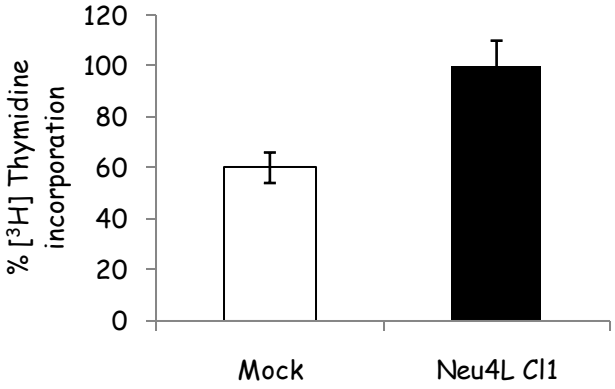

Figure 5.9: % [^{3}H]Thymidine incorporation

5.6.3 MTT ASSAY

As further evidence, mock and Neu4L over-expressing cells were plated and MTT assay was performed every 24hours, as described in materials and methods.

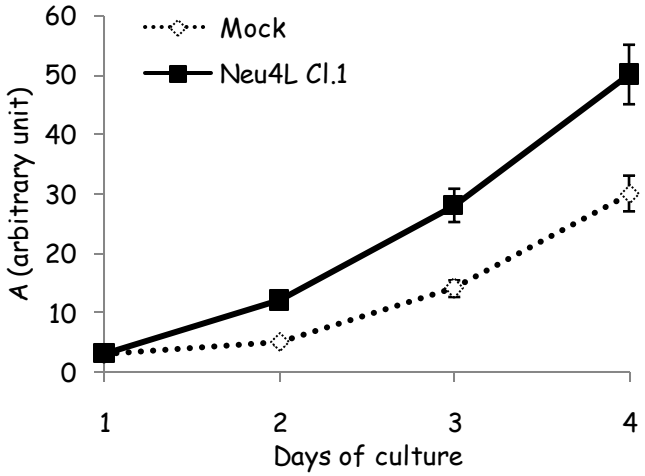

Figure 5.10: MTT assay

Fig. 5.10 shows that cells transfected with Neu4L, were able to convert the chromogenic substrate with an efficiency 1.56-fold higher in comparison to mock cells, confirming an increase of proliferation rate.

5.6.4 SOFT AGAR ASSAY

$1.5x10^5$ Neu4L over-expressing and mock cells were plated, and maintained in soft agar at 37°C and 5% CO_2 for 2 weeks, as described in materials and methods. After, the plates were stained by 0.005% Crystal Violet and incubated for 1 hour.

The colonies formed by Neu4L over-expressing cells were numerically major and larger than colonies formed by mock cells (Fig 5.11).

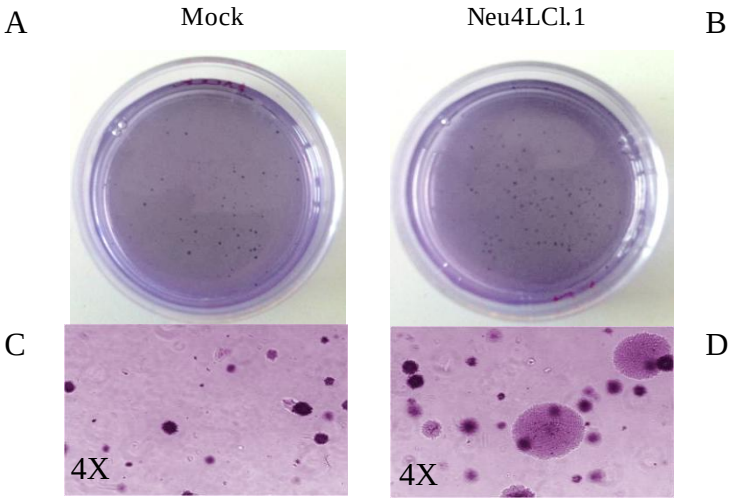

Figure 5.11: Soft Agar assay A) mock colonies B) Neu4L over-expressing colonies C) Phase contrast microphotographas of mock cells and D) of Neu4L over-expressing cells

5.7 NEU4L OVER-EXPRESSION INCREASES THE PHOSPHORYLATION OF RB AND CDK2 PROTEINS

In order to better clarify the changes concerning proliferation rate, previously described, we focused our attention on 2 proteins that are involved in the regulation of cell cycle, Rb and cdk2.

$8x10^5$ mock and Neu4L over-expressing cells were plated in RPMI1640 plus 10 % FBS and 2 mM glutamine and lysed by sonication. The protein content was separated by SDS-PAGE and transferred to PVDF membrane to evaluate Rb and cdk2 phosphorylation.

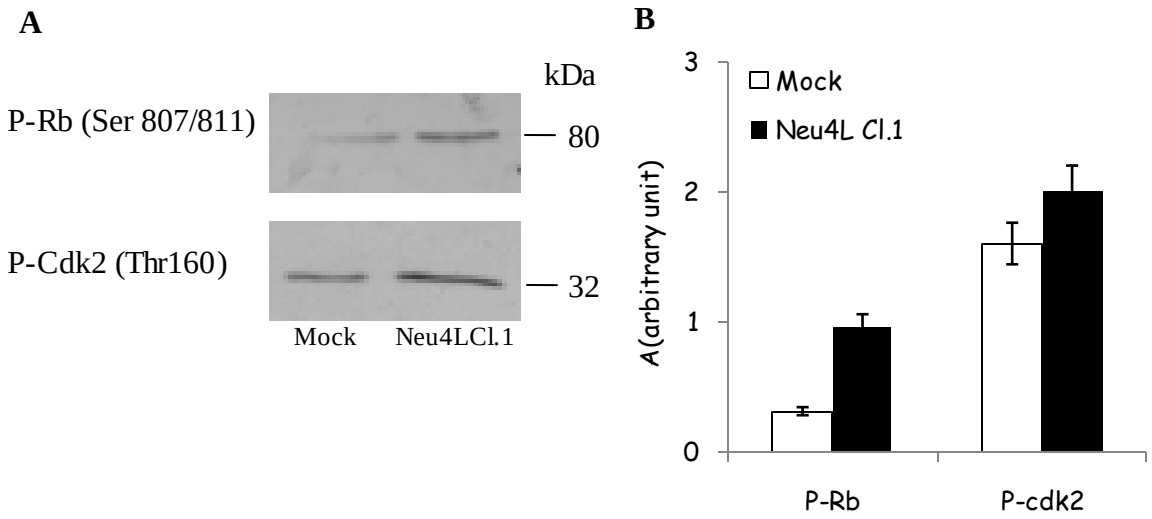

Figure 5.12: A) western blot and B) densitometric analysis of P-Rb and P- cdk2 in mock and Neu4L over-expressing cells

Neu4L over-expressing cells showed a net increase of Rb and cdk2 phosphorylation (Fig. 5.12); in particular, by densitometric analysis, we were able to determine that there was a 3-fold increase of Rb phosphorylation and a 1.24-fold increase of cdk2 phosphorylation, in comparison to mock cells.

5.8 EFFECT OF NEU4L OVER-EXPRESSION ON THE ONCOGENE NMYC

NMYC, as known in the literature, is over-expressed in SK-N-BE cells because of gene amplification (108). We examined possible changes in NMYC gene and protein expression after Neu4L over-expression.

$8x10^5$ mock and Neu4L Cl.1 over-expressing cells were plated in RPMI 11640 plus 10% FBS and glutamine and harvested after 48 hours.

In order to analyze the gene expression, the RNA was extracted and retro-transcribed; to study the protein content, the cells were lysed by sonication, separated by SDS-PAGE, and finally transferred to PVDF membrane.

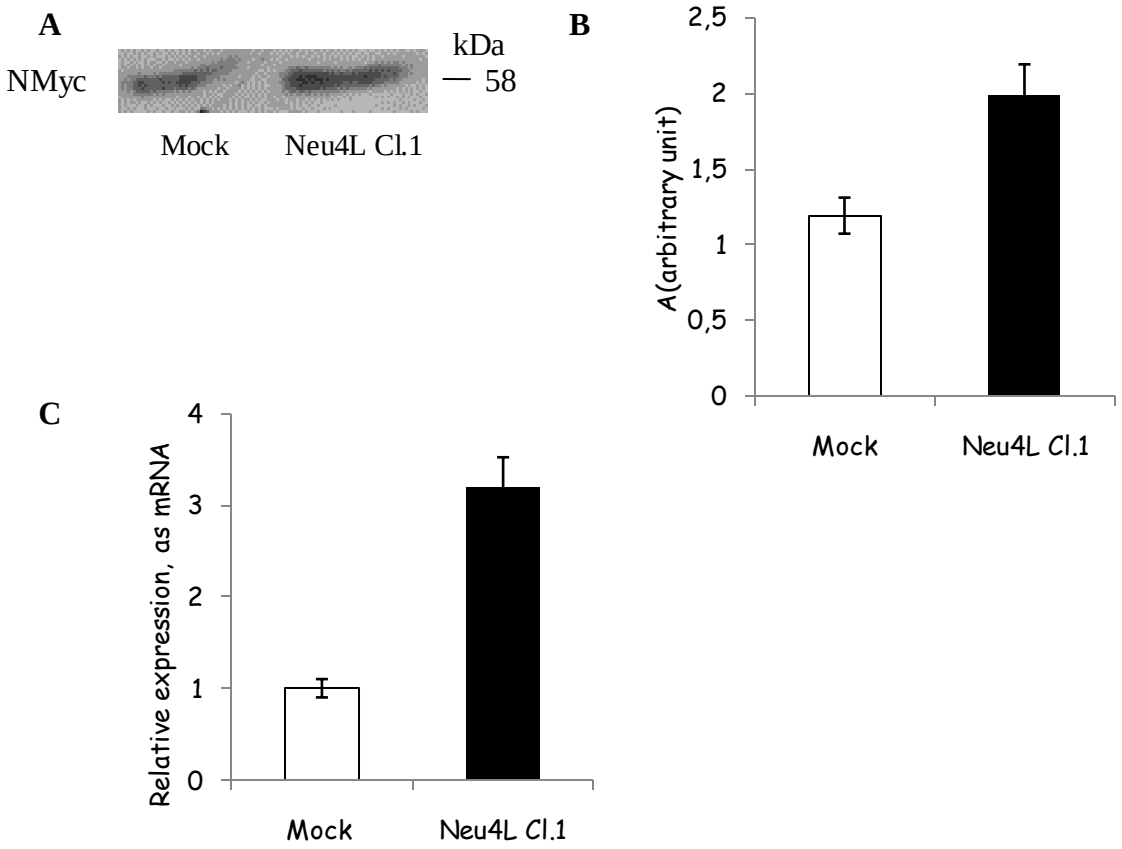

Figure 5.13: Characterization of NMyc: A) western blot of NMyc B) densitometric analysis C) NMYC gene expression by Real-Time PCR

Neu4L over-expressing cells showed a 3-fold increase of NMYC expression and a 1,68-fold increase of protein content in comparison to mock cells.

5.9 EFFECTS OF NEU4L OVER-EXPRESSION ON THE DIFFERENTIATION OF SK-N-BE CELLS

As know in literature, SK-N-BE cells can differentiate along the neuronal lineage under specific stimulation, such as retinoic acid and the reduction of serum (FBS) in the medium (96, 97).

The cells are obliged to not proliferate, but go out from cell cycle and differentiate.

To this end, $6x10^5$ mock and Neu4L over-expressing cells were plated in RPMI1640 plus 1% FBS, and harvested every 24 hours for 6 days. At the 6^{th} day the medium was

replaced with one containing 10% FBS, and the cells were harvested every 24 hours for 3 days.

The differentiation was analyzed by 4 procedures:

1. MTT assay
2. Cell morphology and differentiation markers
3. Analysis of cell cycle by FACS and proteins regulating cell cycle
4. Gene expression of some regulators of cell cycle

5.9.1 MTT ASSAY

Mock and Neu4L over-expressing cells were plated in RMPI 1640 plus 1% FBS up to 6 days; then, the medium was replaced with RPMI 1640 plus 10% FBS.

MTT assay was performed, as described in materials and methods.

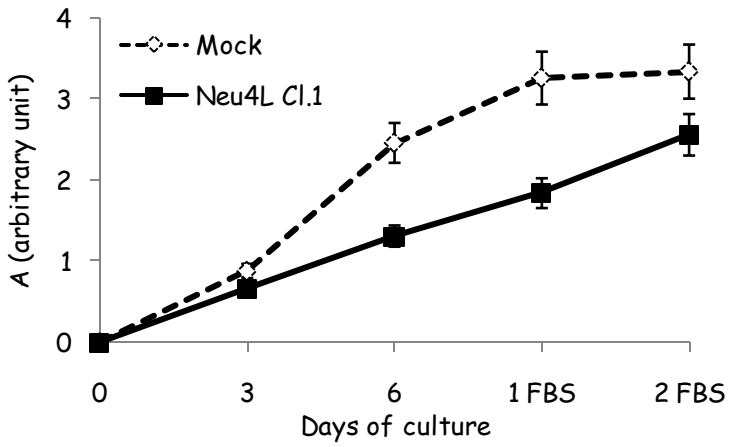

Figure 5.14: MTT assay of mock and NEU4L Cl.1 cells after FBS reduction

Neu4L over-expressing cells seemed to be more sensitive to the reduction of FBS; in fact, they showed a 1.31-fold decrease in comparison to mock cells during the first 3 days of cell culture (Fig 5.14).

This difference increased during the following 3 days of differentiation: at 6th day, Neu4L over-expressing cells showed a 1.88-fold decrease of proliferation rate in comparison to mock cells. When the medium was replaced with one containing 10% FBS, Neu4L over-expressing cells proliferated again more than mock cells. We observed that the difference between mock and Neu4L over-expressing cells was reduced in the following 2 days in 10% FBS (1.88 fold decrease at the 6th day in 1% FBS vs 1.3-fold decrease at the 2nd day in 10% FBS) (Fig.5.14).

5.9.2 CELL MOPHOLOGY AND DIFFERENTIATION MARKERS

Already after 24hours, mock cells tended to establish a dense network of neurites and to undergo to morphological changes such as the reduction of soma, which culminated after 3 days. In contrast, these growth conditions did not suffice to trigger the same process in Neu4LCl.1 cells since the morphological changes and the neurite emission occurred at lower levels than mock cells (Fig. 5.15)

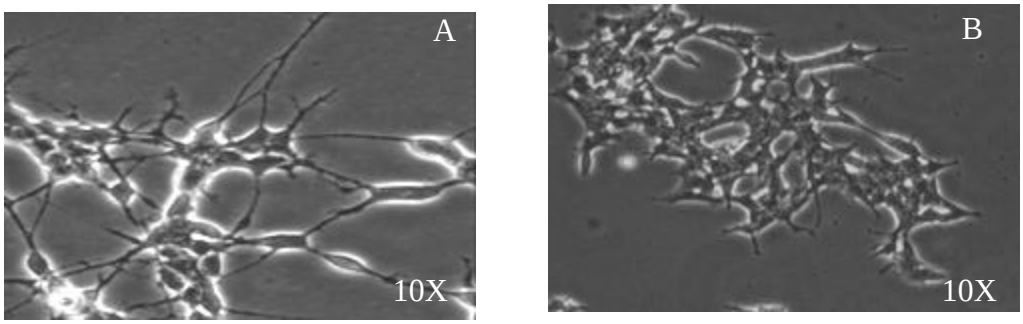

Figure 5.15: Phase contrast microphotographas of A) mock cells B) Neu4L over-expressing cells after 6 days with 1% FBS

In order to evaluate the degree of differentiation, we analyzed two markers of the neuronal differentiation: c-Src and NCAM.

Src family kinase is a family of non-receptor tyrosine kinases that includes nine members. They are involved in many processes in cell biology; in particular c-Src is involved in differentiation (42).

Neural Cell Adhesion Molecule (NCAM, also the cluster of differentiation CD56) is a homophilic binding glycoprotein expressed on the surface of neurons, glia, skeletal muscle and natural killer cells. NCAM has been implicated as having a role in cell-cell adhesion, neurite outgrowth, and synaptic plasticity (154).

In order to value the degree of differentiation $8x10^5$ cells were plated and harvested. The crude homogenate was separated by electrophoresis and transferred to PVDF membrane.

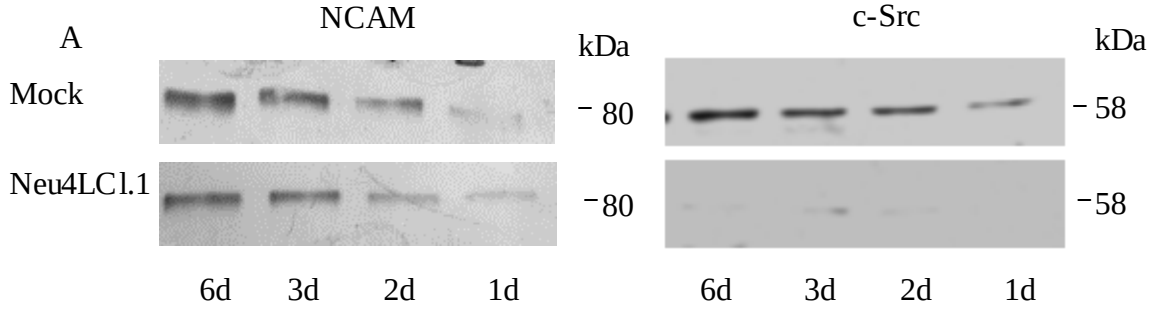

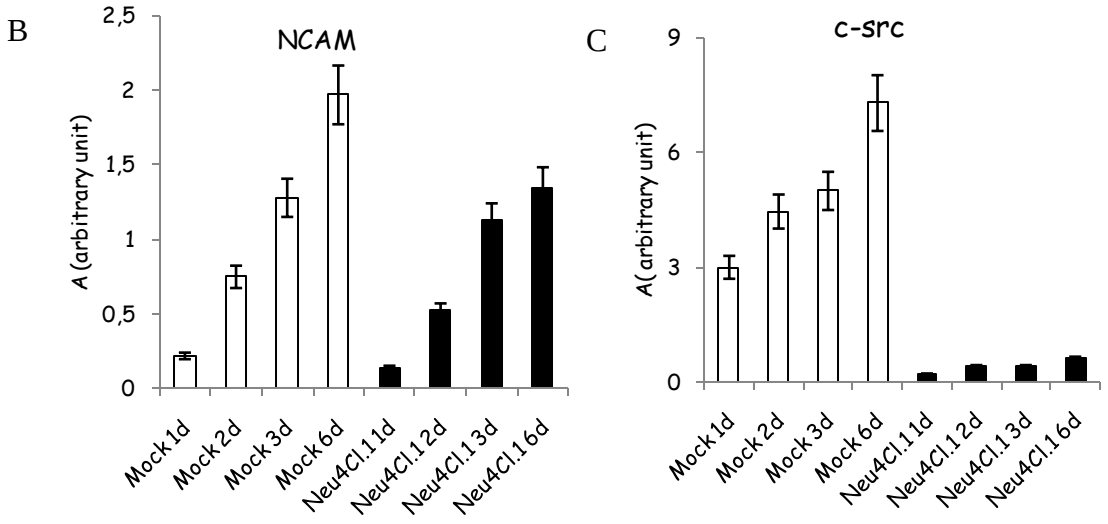

Figure 5.16: A) Western Blot of NCAM and c-Src protein, B) densitometric analysis of NCAM and C) c-Src

Both neuronal markers increased in mock cells during differentiation (Fig. 5.16) and resulted to be less expressed in Neu4L over-expressing cells.

NCAM showed a 1.46-fold decrease in Neu4L over-expressing cells in comparison to mock cells.

c-Src protein was almost absent in Neu4L over-expressing cells. We observed a light increase of the marker at the 6th day, but the levels remained low; instead, in mock cells the level of c-Src protein was higher already at the 1st day and continued to increase until the 6th day.

5.9.3 ANALYSIS OF CELL CYCLE BY FACS

In order to confirm the data obtained through the MTT assay, we decided to investigate the cell cycle by FACS. Mock and Neu4L over-expressing cells were plated, labeled with 20 µM BrdU for 15 min at 37°C, harvested, and fixed in 70% ethanol, as described in materials and methods.

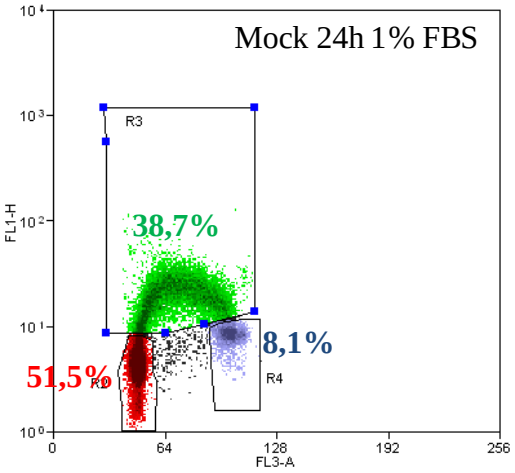
Mock 24h 1% FBS
R3
38,7%
8,1%
51,5%
R2
R4
FL1-H
FL3-A

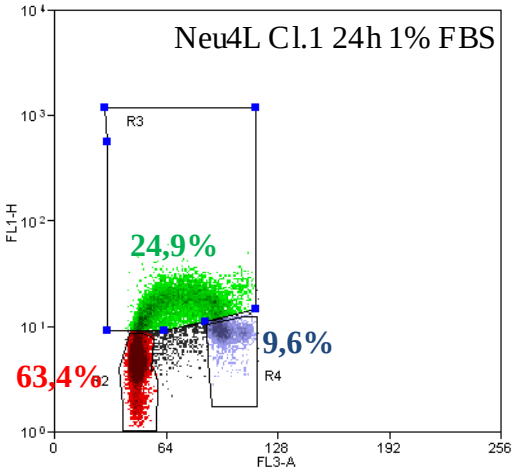
Neu4L Cl.1 24h 1% FBS
R3
24,9%
9,6%
63,4%
R2
R4
FL1-H
FL3-A

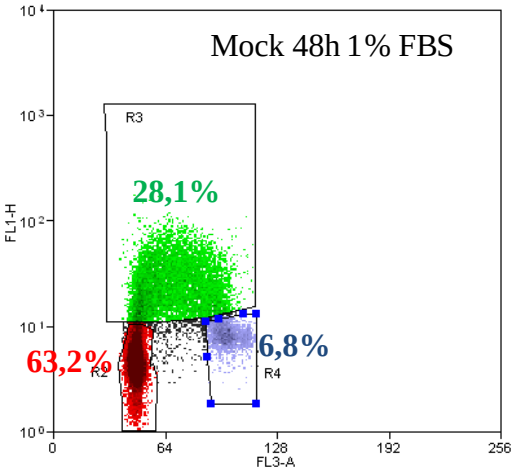
Mock 48h 1% FBS
R3
28,1%
6,8%
63,2%
R2
R4
FL1-H
FL3-A

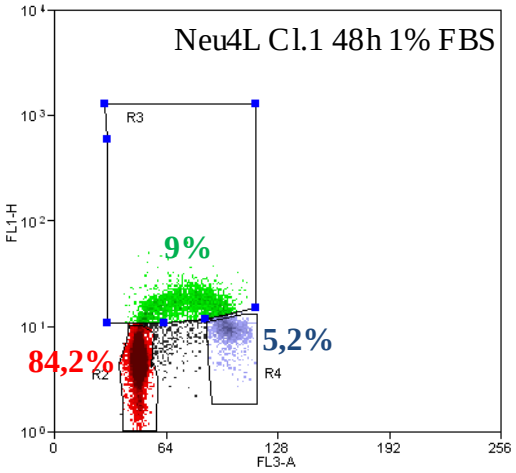
Neu4L Cl.1 48h 1% FBS
R3
9%
5,2%
84,2%
R2
R4
FL1-H
FL3-A

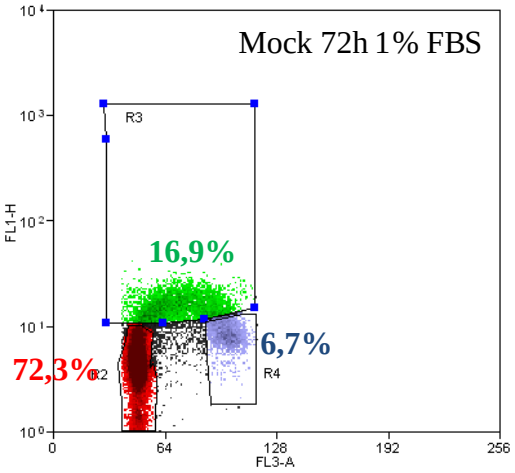
Mock 72h 1% FBS
R3
16,9%
6,7%
72,3%
R2
R4
FL1-H
FL3-A

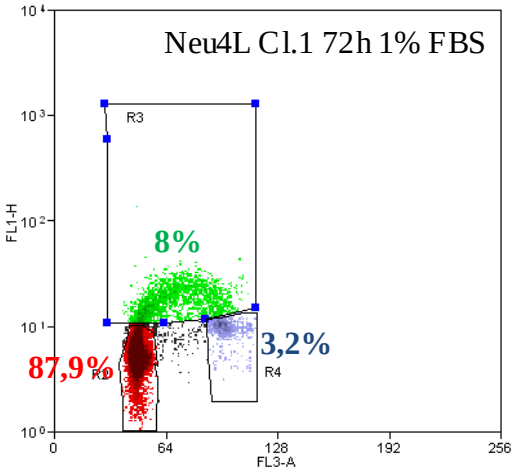
Neu4L Cl.1 72h 1% FBS
R3
8%
3,2%
87,9%
R2
R4
FL1-H
FL3-A

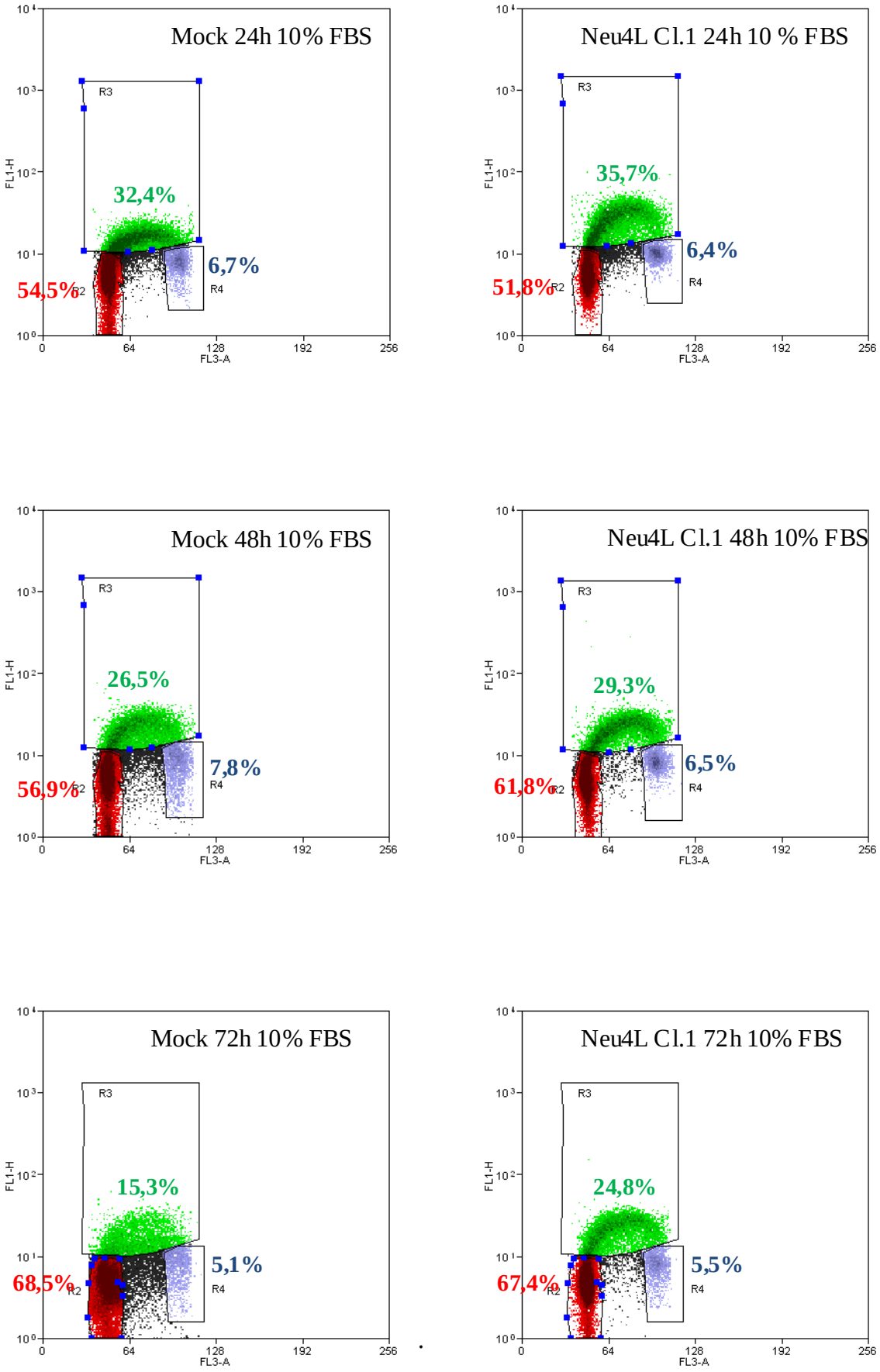

Figure 5.17: analysis of cell cycle by FACS

After 24 hours, 63% of Neu4L over-expressing cells blocked the cell cycle in G1 phase in comparison to 51% of mock cells (Fig. 5.17). This gap increased until the 3rd day of differentiation; in fact, the 88% of Neu4L over-expressing cells were blocked in G1 phase, in contrast to the 71% of mock cells. The block of cell cycle in Neu4L over-expressing cells was annulled when the medium was replaced with RPMI 1640 containing 10% FBS: Neu4L over-expressing cells returned to proliferate and unblock the cell cycle.

It was clear that Neu4L over-expressing cells woke up from a quiescent state and their accumulation in S phase was increased (from 8% at the 6th day in 1% FBS to 35% at 1st day in 10% FBS).

We investigated the behavior of P-Rb and P-cdk2 during the induction of differentiation through serum reduction.

$8x10^5$ cells were plated and harvested. The homogenate crude was loaded on SDS-PAGE and transferred to PVDF membrane.

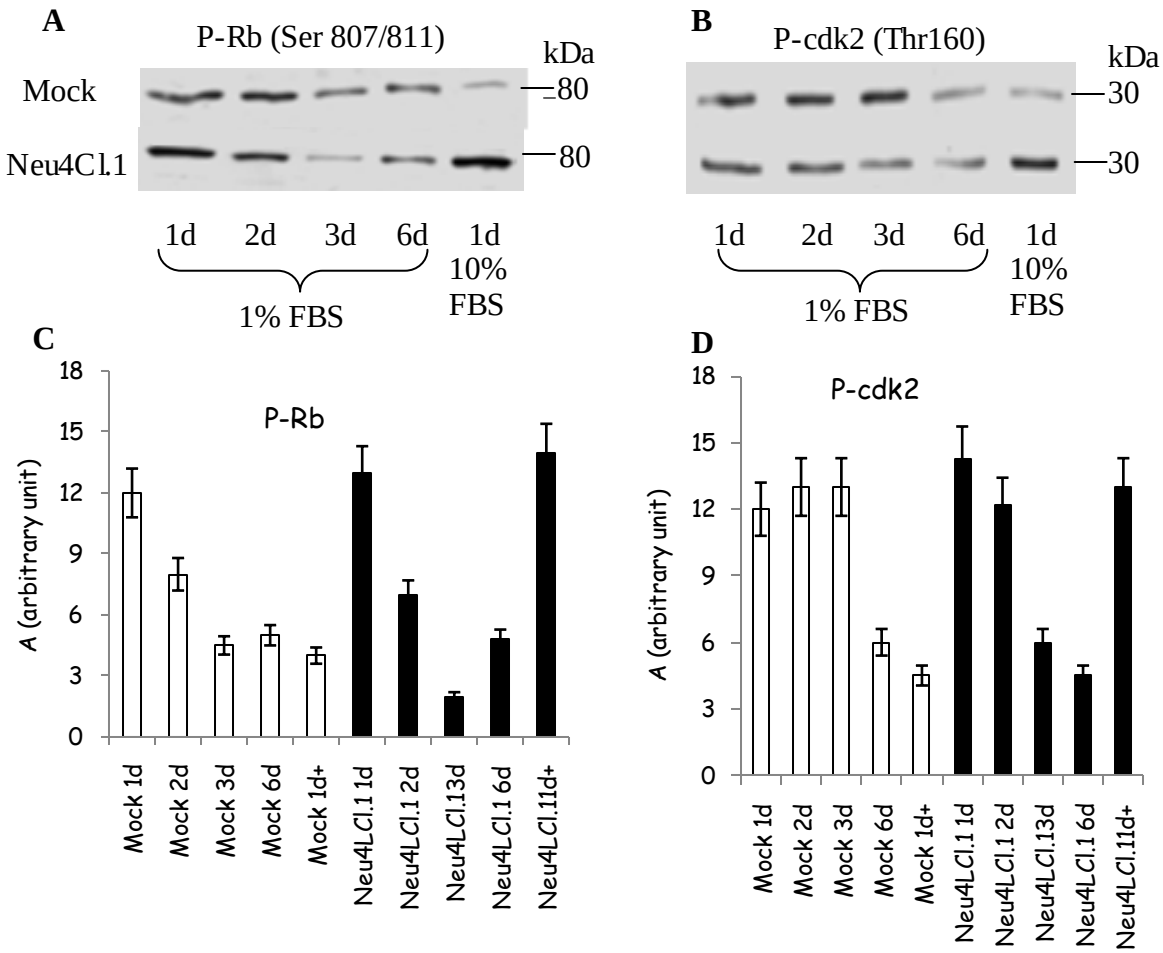

Figure 5.18: A-B) Western Blot of P-Rb and P-cdk2 protein and C-D) densitometric analysis

The content of P-Rb and P-cdk2 changed during differentiation (Fig. 5.18): in Neu4L over-expressing cells, a faster down-regulation of phosphorylation was observed in presence of 1% FBS; at the 3rd day P-cdk2 was 2.2-fold decreased and P-Rb was 2.25-fold decreased in comparison to mock cells. The situation changed, when the medium was replaced with one containing 10% FBS: Neu4L over-expressing cells returned to an initial situation with levels of phosphorylation higher than mock cells (P-cdk2 was 3.5-fold increased and P-Rb was 2.9-fold increased). These data confirmed that the reduction of FBS induced a block of Neu4L over-expressing cells in G1 phase; in fact, the levels of phosphorylation of P-Rb and P-cdk2 decreased. When 10% FBS was added, Neu4L over-expressing cells fully re-activated their proliferation machinery.

5.9.4 REGULATORS OF CELL CYCLE

In order to clarify the alteration on the cell cycle during FBS deprivation, we focused our attention on the gene expression of cyclins, which regulate the G1-S transition, and on inhibitor of cell cycle. In particular, we analyzed the gene expression of:

- Cyclin D1
- p21

The cells were plated, harvested and mRNA was extracted as described in materials and methods, finally, the gene expression was studied by Real-Time.

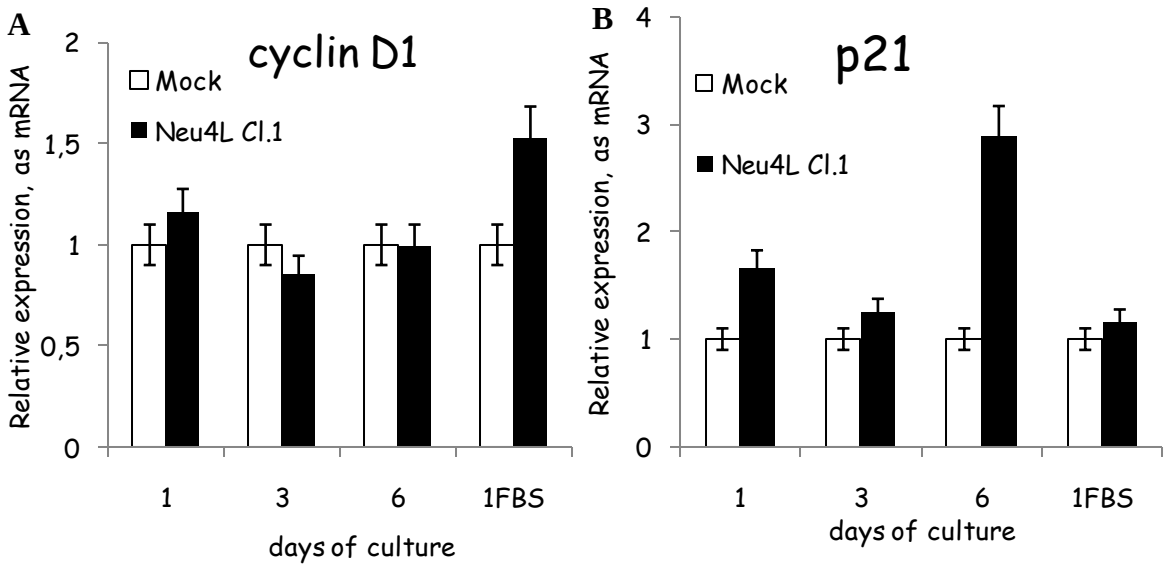

Figure 5.19: Gene expression of CYCLIN D1 (A) and p21 (B) by REAL-TIME PCR

Fig. 5.19 shows that the levels of cyclin D1 slightly decreased during 1% FBS culture but, when 10% FBS was added to culture, its expression showed a 1.5-fold increase in Neu4L over-expressing in comparison with mock cells.

During differentiation, p21expression showed a 1.6-fold increase at the 1st day and a 3-fold increase at 6th in Neu4L over-expressing cells in comparison to mock cells; while, when the medium was replaced with one containing 10% FBS, p21 expression was at the same levels in mock and Neu4L over-expressing cells.

5.10 ACTIVATION OF WNT/β-CATENIN PATHWAY IN NEU4L OVER-EXPRESSING CELLS

We studied the activation of this pathway by 3 different approaches:

1. analysis of active β-catenin content
2. analysis of the activation of β-catenin by luciferase assay
3. analysis of the expression of β-catenin target genes

In order to analyze the β-catenin protein, $8x10^5$ Neu4L over-expressing and mock cells were plated and harvested after 48 hours. The crude homogenate was separated by SDS-PAGE and the proteins were transferred to PVDF membrane.

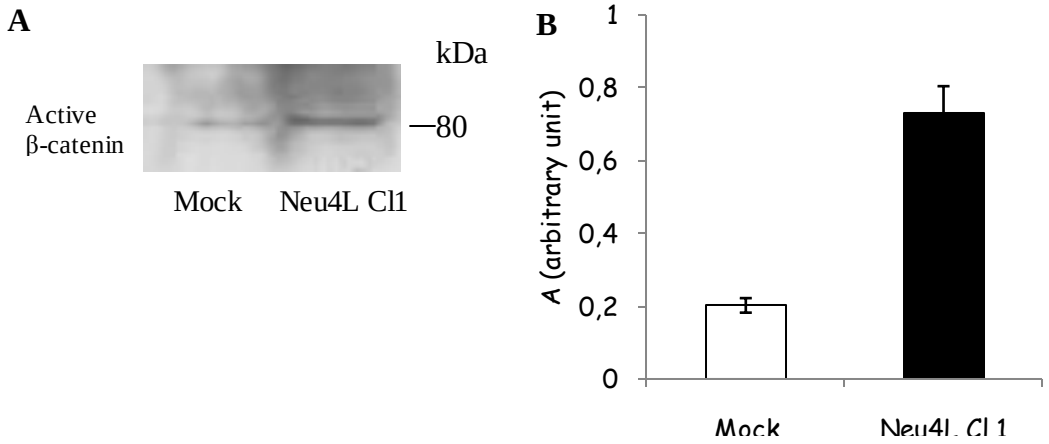

Figure 5.20: A)Western Blot of non-phosphorylated β-catenin and B) densitometric analysis

The amount of active, non-phosphorylated β-catenin was about 3-fold increased in Neu4L over-expressing cells in comparison to mock cells. This data was an indication of the involvement of Wnt/β-catenin pathway (Fig. 5.20).

In order to confirm the previous observations, we used a gene reporter assay responsive to β-catenin.

$6x10^4$ cells were plated and transfected with the TOP-Flash vector; then luciferin was added and the luminescence signal was measured, as described in materials and methods.

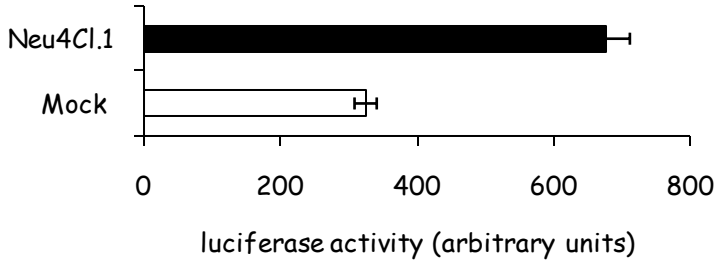

Figure 5.21: TOP-Flash assay in mock and Neu4L over-expressing cells

The Fig. 5.21 shows a 2-fold increase of detected signal in Neu4L over-expressing cells in comparison to mock cells, demonstrating signal the occurrence of a higher gene transactivation activity of β-catenin.

At the end, we focused our attention also on target genes which are regulated by β-catenin activation.

$6x10^5$ cells were plated, harvested, mRNA was extracted and analyzed by Real-Time PCR.

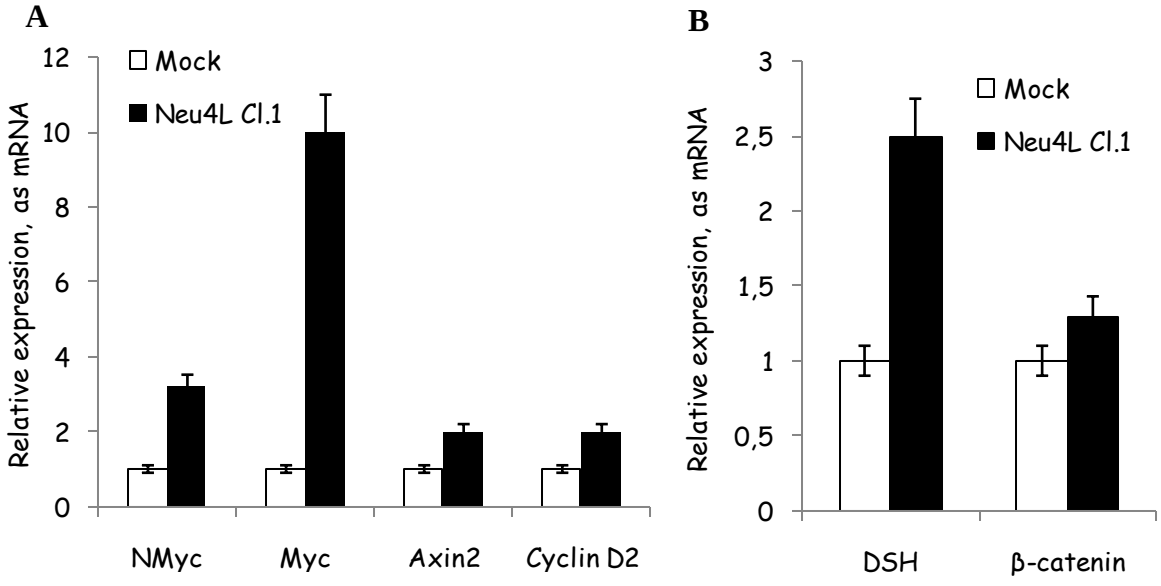

Figure 5.22: A)Real-Time PCR of β-catenin target genes, B9 Real-Time PCR of genes involved in Wnt/β-catenin pathway

Some β-catenin target genes were up-regulated in Neu4L over-expressing cells; in particular we noted that Nmyc was 3-fold increased, myc was 10-fold increased, Axin2 was 2 fold increased, cyclin D2 was 2 fold-increased (Fig.5.22A). We also found that two other genes, involved in Wnt/β-catenin pathway, were up-regulated in Neu4L over-expressing cells: DSH1(Dishevelled 1) was 2.5-fold increased, and, the expression of β-CATENIN was 1.3 fold increased.

5.11 THE TREATMENT WITH LiCl INHIBITS THE DIFFERENTIATION OF SK-N-BE CELLS

LiCl is a well-known activator of Wnt/β-catenin pathway through the inhibition of GSK-β (155).

In order to prove that an increase of β-catenin inhibited the differentiation and induced the modifications identified above in SK-N-BE cells, mock cells were treated with 10 µM LiCl in 1 % FBS medium and then we analyzed:

- the morphological modifications
- the proliferation
- the markers of differentiation

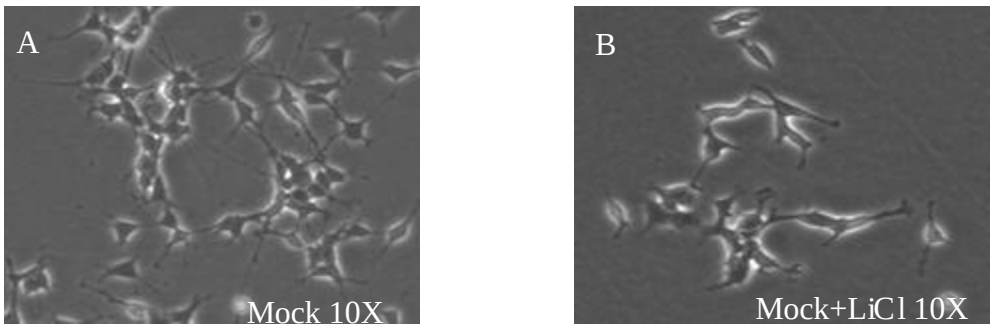

Figure 5.23: Phase contrast microphotographas of A) mock cells B) mock cell + LiCl 10 µM after 3 days of differentiation

After 3 days of culture, mock cells acquired a typical neuronal morphology already described in previous experiments, but mock cells treated with 10µM LiCl presented neurites less developed and also a cell body bigger in comparison to untreated mock cells (Fig.5.23).

For proliferation, mock and mock cells treated with LiCl were plated and MTT was tested at the end of differentiation process, as described in materials and methods.

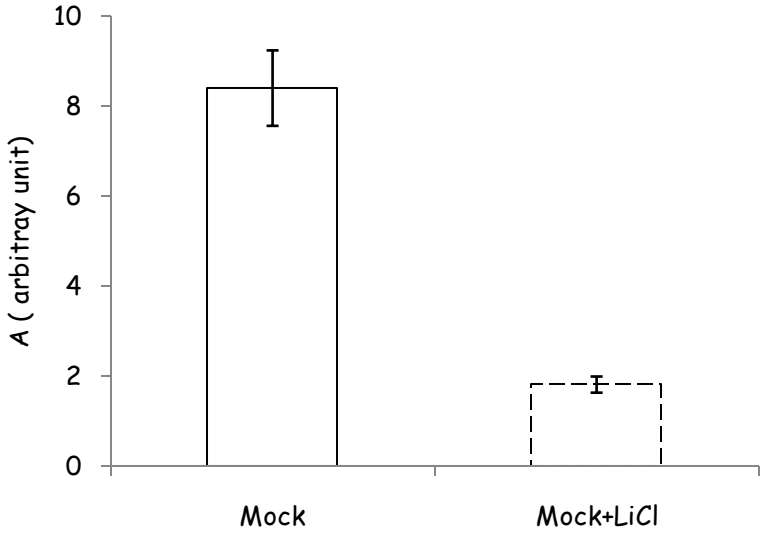

Figure 5.24: MTT ASSAY

MTT assay demonstrated that the treatment of cells with LiCl 10µM induced a 4.6-fold decrease of proliferation in comparison to mock cells (Fig 5.24). This data confirmed that the inhibition of Wnt/β-catenin pathway was involved in differentiation induction.
The morphological and proliferative modifications, described above, induced to think that these cells started to assume a behavior-like Neu4L over-expressing cells.
As further evidence we valued the degree of differentiation after LiCl treatment.
$8x10^5$ cells were plated, harvested and a Western blot was made as described in materials and methods.

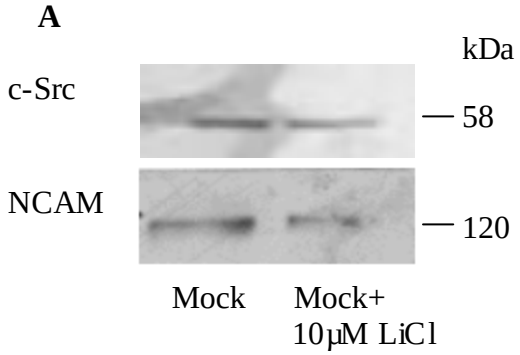

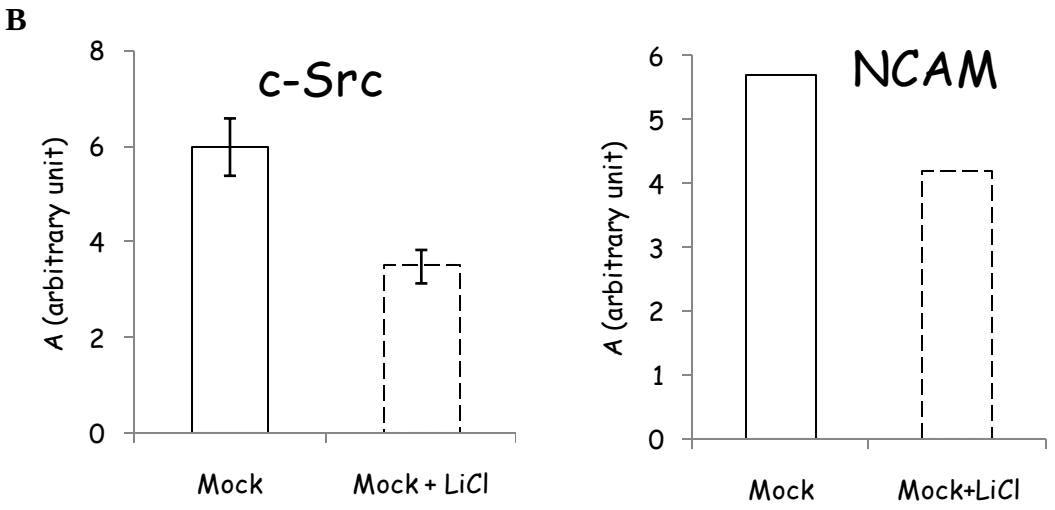

Figure 5.25: A) Western blot and B) densitometer analysis of c-Src and NCAM in mock and mock treated cells with LiCl 10µM

Mock cells showed a 1.7-fold increase of c-Src protein and a 1.3-fold increase of NCAM in comparison to mock cells treated with LiCl (Fig. 5.25). This was another prove that the levels of intracellular β-catenin were crucial to inhibit the differentiation.

5.12 STEM CELL MARKERS

In order to demonstrate that Neu4L over-expression was able to reprogram neuroblastoma cell line, we analyzed the main stem cell markers.

$6x10^5$ cells were plated, harvested and mRNA was extracted as described in materials and methods. The gene expression was studied by Real-Time PCR.

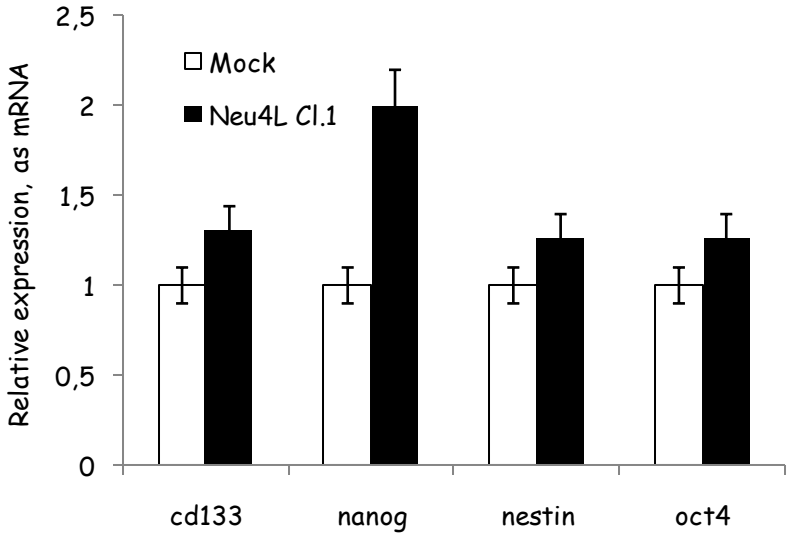

Figure 5.26: Gene expression of stem cell markers

Neu4L over-expressing cells presented higher expression levels of all markers; in particular, CD133, NESTIN and OCT-4 were 1.3 fold increased, while NANOG was 2-fold increased in these cells in comparison to mock (Fig.5.26).

5.13 GLYCOPROTEIC PROFILE

The proteins were fractionated into membrane and cytosol, separated by SDS-PAGE, transferred to PVDF membrane and characterized by using of lectin MAA, which recognizes sialic acid linked $\alpha 2 \rightarrow 3$, and lectin SNA, which recognizes sialic acid linked $\alpha 2 \rightarrow 6$, as described in materials and methods.

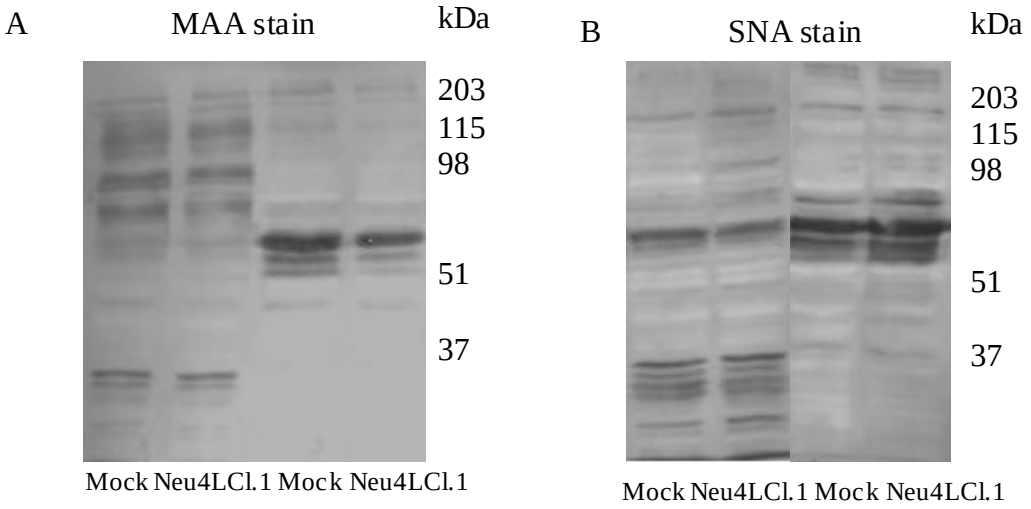

Figure 5.27:Sialoglycoprotein analysis: A) detection with lectin MAA and B) with lectin SNA

The over-expression of sialidase Neu4L induced an important modification on sialoglycoproteins, which were recognized by lectin MAA; these alterations were mainly localized on cytosolic sialoglycoproteins with molecular weight between 51 and 98 kDa; and on membrane sialoglycoproteins with molecular weight about 200 kDa (Fig. 5.27 A).

Instead we did not see considerable modifications on sialoglycoproteins, which were recognized by lectin SNA (Fig. 5.27 B).

5.14 GANGLIOSIDE AND NEUTRAL SPHINGOLIPID PROFILE

Mock and Neu4L over-expressing cells were labeled with [^{3}H] sphingosine, proceeding as described in materials and methods. After a pulse of 2 hours, we calculated that the amount of precursor, which cells incorporated, was equal about 40% -45% of [^{3}H] sphingosine total. After a chase of 24 hours, the cells were freeze-dried; then we have proceeded with the extraction of total lipids and the partition of neutral sphingolipids in an organic phase and gangliosides in an aqueous phase. Lipid extracts, finally, were separated by TLC and quantified with Radiocromatoscanner. The comparison of the ganglioside profile between two cell types did not show significant differences (Fig. 5.28 A, B).

A

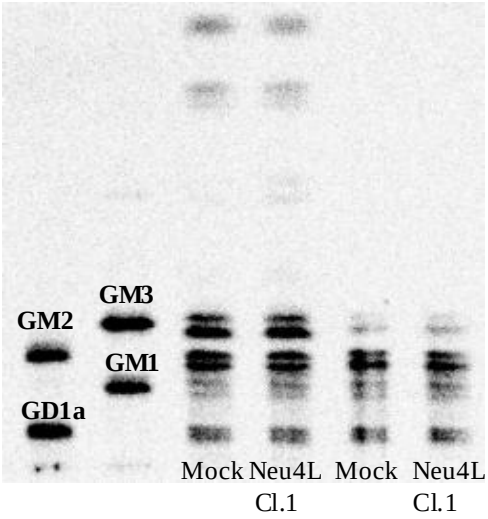

B

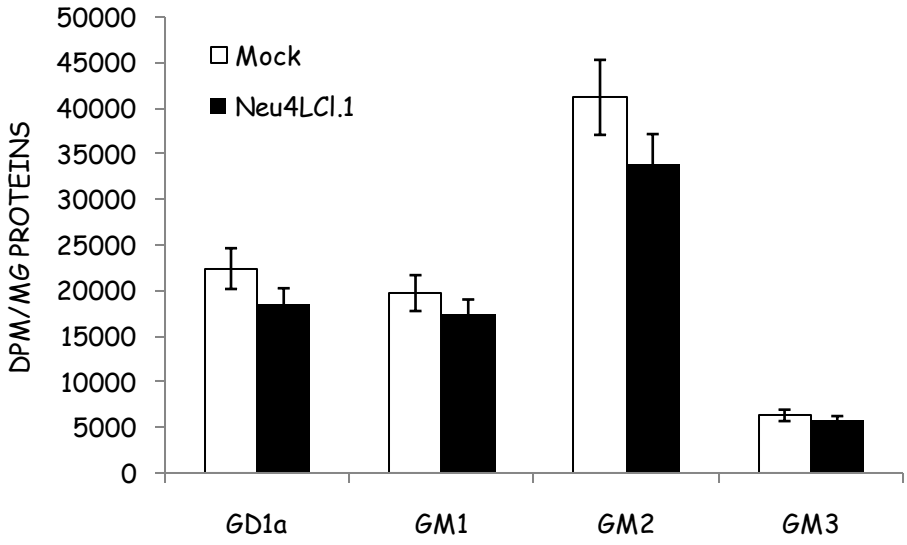

Figure 5.28: A) profile of gangliosides in mock and Neu4L over-expressing cells B) HPTLC gangliosides

Also the profile of neutral lipids did not show significant differences (Fig 5.29 A, B).

A

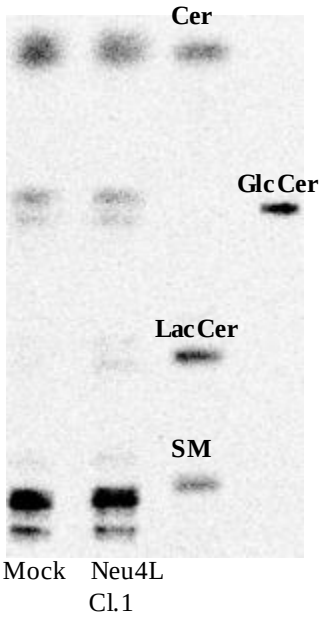

B

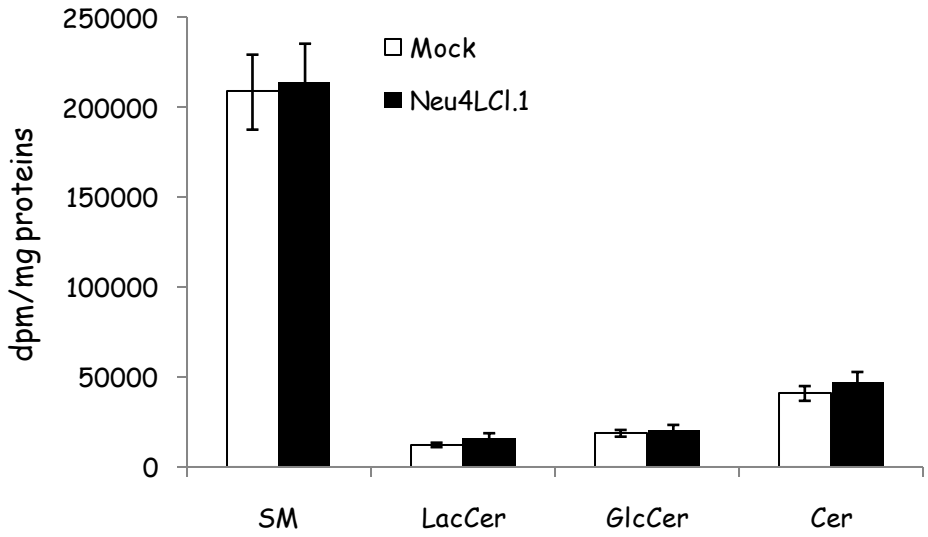

Figure 5.29: A) HPTLC neutral lipid B) profile of neutral lipid in mock and Neu4L over-expressing cells

Moreover, we analyzed cytosolic gangliosides and neutral lipids but we did not find differences in Neu4L over-expressing cell in comparison to mock (Fig 5.29).

A

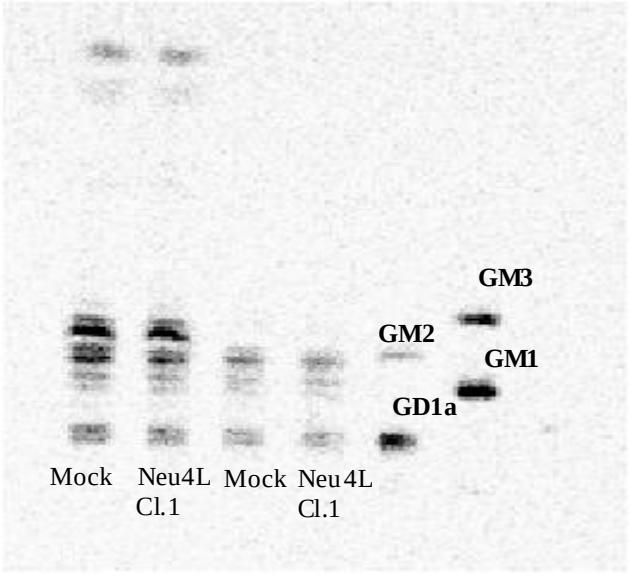
GM3
GM2
GM1
GD1a
Mock
Neu4L Cl.1
Mock
Neu4L Cl.1

B

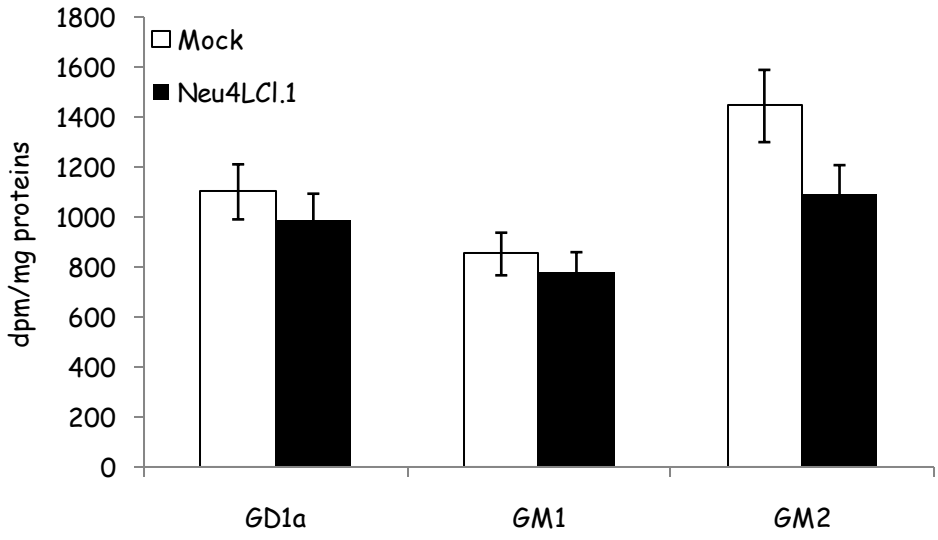
1800
1600
1400
1200
1000
800
600
400
200
0
Mock
Neu4LCl.1
dpm/mg proteins
GD1a
GM1
GM2

C

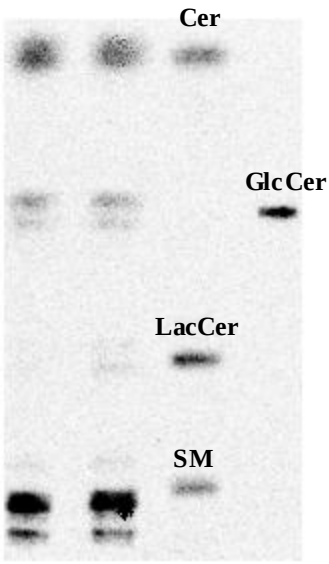
Cer
GlcCer
LacCer
SM
Mock
Neu4L Cl.1

D

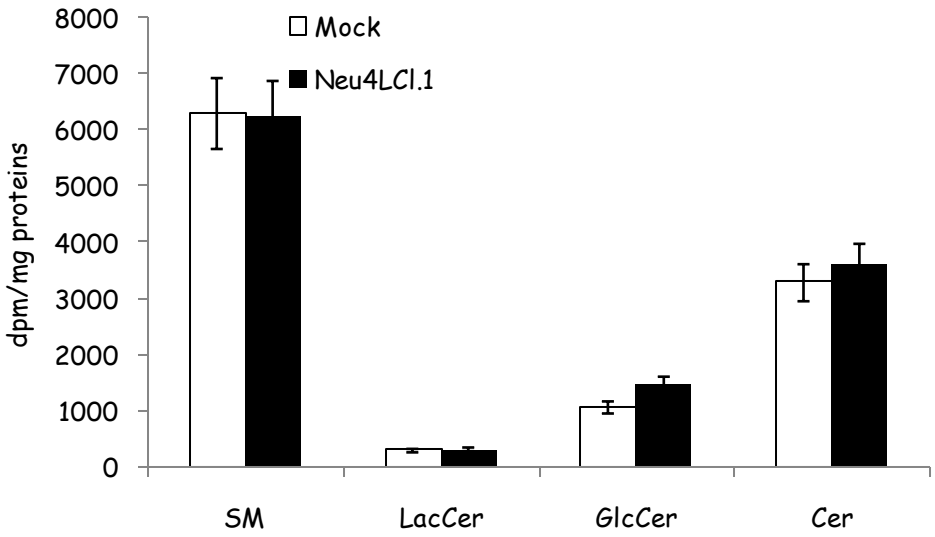

Figure 5.30: A) HPTLC of gangliosides B) profile of gangliosides in mock and Neu4L over-expressing cells C) HPTLC of neutral lipids D)analysis of neutral lipids in mock and Neu4L over-expressing cells

CHAPTER VI

CONCLUSIONS

Cancer transformation is characterized by the occurrence of many processes on glycoconjugates. These phenomena are commonly considered a marker of cancer cells (62). In particular, abnormal glycosylation in pre-malignant lesions and in highly invasive tumours (63) suggests an involvement of abnormal glycoconjugates in neoplastic transformation and in tumor progression, even if the precise role of these molecules has been partially clarified and needs further experimental investigations (68).

In several cases, the aberrant glycosylation process modifies the levels of sialylation and leads to the appearance of altered sialylated glycoproteins and gangliosides (64, 65).

Sialic acid is present in sialoglycoconjugates as a terminal non-reducing residue usually linked to galactose ($\alpha 2 \rightarrow 3$ or $\alpha 2 \rightarrow 6$), and to N-acetylgalactosamine or N-acetylglucosamine ($\alpha 2 \rightarrow 6$); moreover, the sialic acid chains may be present as terminals, or wire internal saccharide residues into glycolipids and glycoproteins.

It is known that an increase of sialic acid content is related to malignant the phenotype, and to the capacity of invasion and the metastatic potential of cancer cells (16).

Moreover, cancer gangliosides are present on cell membranes and secreted in large quantities in comparison to normal gangliosides (68). These gangliosides play a key role in the cancer progression; in fact, they strongly regulate the cell adhesion/motility and induce immune-suppression in the organism (68).

Also, in the carbohydrate portion of glycoproteins are found changes related to neoplastic transformation and, in particular, an increase of sialic acid content is often reported (64). The alteration of membrane glycoproteins, such as selectins and integrins, is functionally important for the cell and is reflected in the adhesion properties and motility of cancer cells, with consequences on the growth and metastatic potential of tumor (64).

The levels of sialylation of glycoproteins and gangliosides are mainly determined by the activity of two categories of enzymes: sialidases and sialyltransferases.

The evidences of sialyltransferases' involvement in malignant disease are still low, while there are proofs that suggest an active participation of sialidases in determining the malignant phenotype (16).

Human sialidases are four and are classified on the basis of their localization and specificity of substrate:

1. lysosomal sialidase Neu1 (4)
2. cytosolic sialidase Neu2 (22)
3. membrane sialidase Neu3 (55)
4. mitochondrial or inner membrane sialidase Neu4 (48, 49)

Among these enzymes, the last to be discovered and still partially unknown is Neu4 (49).

Much interest has aroused on this enzyme because NEU4 gene is expressed in two isoforms: the Neu4Long form (Neu4L), which presents a sequence of 12 amino-acid at the N-terminal, as signal sequence for mitochondrial localization, and the Neu4Short form (Neu4S), which is ubiquitously expressed and associated with inner cell membranes (48).

The role of Neu4 is still unclear, but recent studies show the involvement of Neu4S in the modulation of metastatic behavior (49), in particular in colon tumor.

To the contrary, the study of Neu4L is more complicated; in fact, its physiological role is still unknown, but it was demonstrated its involvement in mitochondrial signaling, such as apoptosis (50), and in neuronal differentiation (82). Moreover, Neu4L resulted to be scarcely expressed in adult tissue, in contrast to fetal tissue and nervous system during development. We characteristically found a high expression of Neu4L also in neuroblastoma cell lines.

In light of these considerations, we developed a research project to clarify if Neu4L could play a role in neuroblastoma pathogenesis.

We used two cellular models: the SK-N-BE cells, which carry the amplification of the oncogene MYCN and a greater degree of malignancy, and the SH-SY5Y cells, without MYCN amplification(106).

Preliminary investigations showed a 3.57-fold increase of Neu4L expression in SK-N-BE cell line in comparison to SH-SY5Y (Fig. 5.1).

In order to identify the meaning of a possible involvement of Neu4L in the pathogenesis of neuroblastoma, it was decided to over-express Neu4L in SK-N-BE cell line.

After transfection and selection of clones, we quantified the increase of Neu4L by gene expression and sialidase activity assay.

The results indicated that Neu4L clone 1 showed a 1,700-fold increase, as gene expression, in comparison to mock cells (Fig. 5.2). Also, sialidase activity at pH 3.2 was 1.83-fold increased in Neu4L over-expressing cells (Fig. 5.3). Moreover, we also tested the sialidase activity against fetuin, as representative sialoglycoproteins, and we found that Neu4L over-expressing cells showed a 1.4-fold increase in comparison to mock cells at pH 3.2 and pH 7 (Fig. 5.4). These data indicated that the over-expression of Neu4L was successful and sialidase was also active at physiological pH.

The most significant data concerned the impact of Neu4L on the phenotype and physiology of cells, transfected with vector pcDNA 3.1-myc-Hys Neu4L. First, the over-expression of Neu4L induced deep changes in the cell proliferation.

In order to demonstrate this modification, several tests were carried out: a) a growth curve showed a 1.56-fold increase in Neu4L over-expressing cells in comparison to mock cells (Fig. 5.8); b) the incorporation of [^{3}H] thymidine showed a 1.58-fold increase in Neu4L over-expressing cells in comparison to mock cells (Fig. 5.9); c) the MTT test revealed that Neu4L over-expressing cells were more able (1.56-fold) to convert the chromogenic substrate than the mock controls (Fig.5.10); d) the Soft Agar assay demonstrated that Neu4L over-expressing colonies were numerically more and larger than mock cells (Fig. 5.11). All these proofs demonstrated that the over-expression of Neu4L induced an increase of proliferation rate. In accordance with these data, we demonstrated the inhibition of main regulator of cell cycle, Rb, in parallel to the up-regulation of cdk2.

The retinoblastoma protein, Rb, is a tumor suppressor protein that is dysfunctional in many types of cancer. One highly studied function of Rb is to prevent excessive cell growth by inhibiting cell cycle progression until the cell is ready to divide. Rb prevents the cell from replicating damaged DNA by preventing its progression along the cell cycle through G1 into S (156). Through the inhibition of transcription factors of the E2F family. In the hypophosphorylated state, Rb is active and carries out its role as tumor suppressor by inhibiting cell cycle progression. Phosphorylation inactivates Rb (156).

Cdk2 (cyclin-dependent kinases 2) belongs to a family of serine/threonine kinases activated by cyclins In the late G_1 phase, Cdk2 is activated by binding to cyclin E and completes the phosphorylation of Rb leading to further activation of E2F mediated transcription (157). This leads to passage through the restriction point at the boundary

of the G_1/S phase, and to S phase initiation. Later, Cdk2 plays an important role in S phase progression by binding with cyclin A (157).

We found that the phosphorylated forms of these proteins, Rb and cdk2, were increased in Neu4L over-expressing cells (Fig. 5.12). These data demonstrated that the increase of proliferation rate was due to a higher transition from G1 to S phase of cell cycle.

Moreover, we observed that Neu4L over-expression induced a marked increase in NMYC mRNA and protein expression (Fig. 5.13). As repeatedly emphasized throughout this thesis, the expression of NMYC determines the malignancy and stage of neuroblastoma. In that way, the over-expression of NMYC is able to overturn the regulation of the cell (107). Its main role is to regulate the entrance in G1 phase to accelerate the shift in S of the cell cycle (107). All these observations demonstrated that the increase of cell proliferation was due to a de-regulation of cell cycle by accelerating the transition from G1 to S phase.

A second effect of Neu4L over-expression concerned SK-N-BE differentiation.

One of methods, more used to induce differentiation, was plated cells in presence of 1% FBS.

After inducing differentiation by reduction of FBS, we observed that Neu4L over-expressing cells were not able to assume a neuronal morphology, but they maintained a cell body somewhat around with few neuronal processes (Fig. 5.15).

In order to confirm our observations, described above, we studied two of main neuronal markers: c-Src and NCAM

c-Src tyrosine kinase, also known as CSK, includes an SH2 domain, an SH3 domain and a tyrosine kinase domain (42). It was demonstrated that c-Src expression increase during neuronal differentiation (42).

NCAM, Neural Cell Adhesion Molecule, is a homophilic binding glycoprotein expressed on the surface of neurons, glia, skeletal muscle and natural killer cells (154). NCAM has been implicated as having a role in cell-cell adhesion, neurite outgrowth, synaptic plasticity, and learning and memory (154).

After inducing differentiation, we noted that both c-Src and NCAM proteins increased in mock cells in contrast to Neu4L over-expressing cells (Fig 5.16). This was incontrovertible evidence that the over-expression of Neu4L inhibited the differentiation

process; while mock cells were able to trigger neuronal differentiation also in terms of neurites emission.

Moreover, serum reduction induced a singular reaction in Neu4L over-expressing cells; in fact, we decided to analyze cell cycle by FACS and we noted that they arrested nearly completely their growth, but did not die (data non shown), entering in a sort of quiescent state and fully re-activating the proliferation machinery as soon as the 10% FBS was re-added to the culture medium, as a mechanism of defense to preserve cell survival. We noted that there was a net accumulation of Neu4L over-expressing cells in G1 phase until the 3rd day of differentiation (88% Neu4L vs 71% mock), while the situation changed when the medium was replaced with one containing 10% FBS; in fact these cells passed from a quiescent to a vital state, increasing their accumulation in S phase (Fig 5.17).

The block in a quiescent state was confirmed through MTT assay; in fact, after 6 days in 1% FBS, Neu4L over-expressing cells showed a 1.8-fold decrease of proliferative rate in comparison to mock cells; but when the medium was replaced with one containing 10% FBS, Neu4L over-expressing cells started again to proliferate more rapidly than mock cells (Fig. 5.14).

These observations were also confirmed analyzing the cyclin D1 and the inhibitor of cell cycle p21. As expected, over-expression of Neu4L induced changes of parameters which are involved in the block of cell cycle; in fact, we identified a decrease of cyclin D1 and an increase of p21 in Neu4L over-expressing cells, in comparison to mock cells (Fig. 5.19). We did not find significant modifications on gene expression of apoptotic genes(data not shown). These proofs demonstrated that over-expression of Neu4L blocked cell cycle during serum withdrawal but it did not activate the apoptosis pathway.

Another validation of this trend was given analyzing the phosphorylated forms of Rb and cdk2 during serum deprivation. As described above, in presence of 10% FBS, their phosphorylation increased in Neu4L over-expressing cells in comparison to mock; instead we noted that, during serum deprivation, the phosphorylated forms of cdk2 and Rb dramatically decreased in Neu4L over-expressing cells in comparison to mock cells. When the medium was replaced with one containing 10% FBS, the situation changed

again; in fact, Neu4L over-expressing cells increased the levels of Rb and cdk2 phosphorylation in comparison to mock cells (Fig. 5.18).

All these data confirmed that Neu4L, during the reduction of FBS, moved the cells to a quiescent state, in which cells did not answer to outer stimuli but stayed in a "standby state".

It is known that one of the most important pathways, which regulates the balance between proliferation and differentiation, in neural crest from which neuroblastoma arises, is Wnt/ β-catenin (137). In condition of inactivated signaling, intracellular β-catenin is bound to a complex of proteins (137), which induces its degradation (138-141); in contrast, the binding of Wnt to its receptor activates an intracellular signaling which causes the dephosphorylation of β-catenin and its translocation to the nucleus (136).

Our results showed that Wnt/β-catenin pathway was more activated in Neu4L over-expressing cells that in mock cells. This event was demonstrated by analysis of active, non-phosphorylated β-catenin and by a luciferase gene reporter assay responsive to β-catenin (Fig. 5.21).

All data confirmed that there was a major activation of β-catenin in Neu4L over-expressing cells and could explain the proliferative alteration described above. Moreover, we analyzed the modifications of β-catenin expression of target genes (NMYC, MYC, AXIN2 and CYCLIN D2) which are involved in progression of cell cycle (138-141). An up-regulation of all these genes was present, and these proofs further demonstrated that Wnt/β-catenin pathway was more active in Neu4L over-expressing cells and that this activation could induce modifications in cell proliferation (Fig. 5.22A). We also investigated gene expression of DSH (138-141) and β-CATENIN, which increased in Neu4L over-expressing cells in comparison to mock cells (Fig. 5.22B).

It is known that the accumulation of intracellular β-catenin is able to induce block of differentiation (150, 151). To confirm that also in our cells the activation of the β-catenin signaling could be related to the behavior of Neu4L over-expressing cells in 1% FBS, we treated mock cells with an inhibitor (LiCl) of GSK3β, which is responsible of β-catenin degradation (155), in order to activate Wnt/β-catenin pathway.

LiCl treated mock cells were unable to trigger neuronal differentiation in terms of neurites emission and appearance of markers (c-Src and N-CAM), under reduction of FBS (Fig 5.25). Moreover, they blocked their proliferation more significantly than non-treated mock cells, in similar way to Neu4L over-expressing cells (Fig. 5.24).

It is known in literature that most of proteins, involved in Wnt/β-catenin pathway such as also inhibitors, are glycoproteins (137). Can the alteration on one of these "characters" modify cell proliferation and differentiation of SK-N-BE cell line?

As described above, Neu4L, in vitro, recognized fetuin, a sialo-glycoprotein, also at a neutral pH. Moreover, it was able to induce, in vivo, deep modifications on some cytosolic sialo-glycoproteins, in the range of 50-60 KDa, and on membrane sialo-glycoproteins at 80 and 100 KDa; instead, we did not find Neu4 sialidase activity towards ganglioside in vitro and in vivo (Fig. 5.27).

The localization of Neu4L was found in mitochondria and RER (48, 49) (Fig. 5.6). These data suggested that the Neu4L activity is direct on intracellular sialo-glycoproteins.

Our hypothesis is that the alterations on cell proliferation and differentiation are due to the action of Neu4L on one or more sialo-glycoproteins, which are involved in the activation of Wnt/ β-catenin signaling.

In summary, we describes Neu4L as a possible regulator of malignancy in SK-N-BE through the promotion of Wnt/β-catenin pathway, which induces modification in cell proliferation and the de-differentiation of tumoral cells.

As last observation we found an increase of some stem cell markers in Neu4L over-expressing cells, which are correlated with a poor prognosis, and are linked to a phenotype like-stem cell induced by the activation of Wnt/β-catenin signaling (25).

These finding could open new and important input in clinical application in Neuroblastoma, employing Neu4L expression as a prognostic marker.

CHAPTER VII

BIBLIOGRAPHY

BIBLIOGRAPHY

1) Monti E. et al. (2002) Neurochem. Res. **27**, 649-663
2) Komandoor E. et al. (2001) Comp. Biochem. and Physiol., part B **129**, 29-64
3) Corfield T. (1992) Glycobiololy **2**, 509-512
4) Miyagi T. et al. (2002) Int. J. Cancer **97**, 180-185
5) Lukong E. et al. (2001) J. Biol. Chem. **276**, 46172-46181
6) Jaurousse N. et al. (2000) Traffic **1**, 378-384
7) Dell'Angelica E.C. et al. (1999) Mol. Cell. **3**, 11-21
8) Ostrov D.A. et al (2000) Science **290**, 816-819
9) Tringali C. et al. (2004) J. Biol. Chem. **279 (17)**, 16989-16995
10) Naraparaju V.R. et al. (1994) Immunol. Lett. **43**, 143-148
11) Cross A.S. et. al. (1991) J. Clin. Invest. **88**, 2067-76
12) Bonten E. et al. (1996) Genes Dev. **10**, 3156-3169
13) Pshezhetsky A.V. et al. (1996) J. Biol. Chem. **271**, 28359-28365
14) Hiraiwa M. et al. (1997) Biochim. Biophys. Acta **1341,** 189-199
15) Potier M. et al. (1990) Biochem. J **267**, 197-202
16) Miyagi T. et al (2004) Glycoconj. J. **20**, 189-198
17) Okamura-Oho Y. et al (1994) Biochim Biophys Acta **1225(3)**; 244-254
18) Suzuki K. (1995) Nippon Rinsho **53(12),** 2887-2891
19) D'Azzo A. et al. (1982) Proc. Natl. Acad. Sci **79**, 4535-4539
20) Rudenko G. et al. (1995) Structure **3(11),** 1249-1259
21) Arai Y. et al. (1999) Ultrastruct. Pathol. **23(6),** 369-374
22) Monti E. et al. (1999) Genomics **57**, 137-143
23) Sato K. et al. (1996) Biochem. Biophys. Res. Commun. **221**, 826-830
24) Olson E.N. et al. (1994) Genes Dev. **8**, 1-8
25) Sato K. et al (1995) Glycobiology. **5**, 511-516
26) Akita H. et al (1997) Histochem. Cell. Biol. **107**, 495-503
27) Fanzani A. et al (2003) FEBS. Lett. **547 (1-3)**, 183-188
28) Tokuyama S. et al. (1997) Int. J. Cancer **73**, 410-415
29) Zanchetti G. et al. (2007) Biochem. J. **408,** 211-219
30) Kalka D. et al. (2001) Biochem. Biophys. Res. Commun. **283**, 989-993
31) Simon K. et al. (1997) Nature **387**, 569-572
32) Tettamanti G. et al. (1993) Adv. Lipid Res. **25,** 235-267

33) Kopitz J. et al. (1996) Glycobiology **6**, 367-376

34) Wang Z. et al. (2002) J. Biol. Chem. **277,** 26252-26259

35) Proshin S. et al (2002) Neurochem. Res. **27**, 841-846

36) Rodriguez J. A. et al. (2001) J. Neurosci. **21**, 8387-8395

37) Da Silva J. S. et al (2005) Nat. Neurosci. **8**, 606-615

38) Saito M. et al. (1992) J. Neuroch em. **58**, 83-87

39) Kopitz J. et al. (2001) FEBS Lett. **491,** 233-236

40) Pitto M. et al. (1989) J. Neurochem. **53**, 1464-1470

41) Wu G. et al. (1995) J. Neurochem **65(3),** 1419-1422

42) Valaperta R. et al. (2007) J. of Neurochem. **100**, 708-719

43) Da Silva J. S. et al. (2005) Nature Neuroscience **8**, 606-615

44) Miyagi T. et al. (2008) Proteomics **8**, 3303-3311

45) Sasaki A. et al. (2003) J. Biol. Chem. **278 (30)**, 27896-27902

46) Moon S.K. et al. (2007) Biochem. Biophys Res. Common **356(3),** 542-547

47) Papini N. et al. (2004) J. Biol. Chem. **279 (17)**, 16989-16995

48) Yamaguchi K. et al. (2005) Biochem J., **390**: 85-93

49) Monti E. et al. (2004) Genomics **83**, 445-453

50) Miyagi T. et al (2007) Federat. Europ. Biochem. Soc. **581**, 406-412

51) Finlay T. M. et al. (2010) Glycoconj. **27**, 329-348

52) Finlay T. M. et al. (2010) Glycoconj [Epub ahead of print]

53) Milner C.M. et al. (1997) J. Biol. Chem. **272,** 4549-4558

54) Murre C. et al. (1989) Cell **56**, 777-784

55) Monti E. et al. (2000) Biochem. J. **349**, 343-351

56) Miyagi T. et al. (1993) J. Biol. Chem. **268**, 26435-

57) Roggentin P. et al. (1989) Glycoconj J. **6**, 349-353

58) Schauer R. (1985) Trends Biochem. Sci. **10**, 357-360

59) Fronda C. L. et al. (1999) Biochem Biophys. Res. Commun. **258**, 727-731

60) Roggentin P. et al. (1993) Mol. Microbiol. **9**, 915-921

61) Schauer R. et al. (1984) Hoppe Seylers Z. Physiol. Chem. **365**, 419-426

62) Hakamori S. (2002) Proc. Natl. Acad. Sci **99**, 10231-10233

63) Fogel M. et al. (1983) J. Exp. Med. **157,** 371-376

64) Ladler P. (1997) Acta Biochem. Pol **44(2**); 343-357

65) Basu S. et al. (1995) Biology of the sialic acid pp 69-94, Rosemberg A. ed, Plenium Press New York

66) Hakamori S.I. et al. (1996) Cancer Res. **56**, 5309-5318

67) Hakamori S.I. (1984) Trends Biochem Sci. **9,** 453-459

68) Sakawa M. et al. (2002) Int. J. Cancer **97**, 180-85

69) Miyagi T. et al. (1994) FEBS Lett. **349**, 255-259

70) Kato T et al. (2001) Int. J. Cancer **94**, 797-804

71) Gillar B.K. et al. (1993) Glycobioogy. **3**, 57-67

72) Emmanueille J. et al. (1999) Cancer Res. **59**, 234-240

73) Tringali C. et al. (2007) J. Biol. Chem. **282**, 14364-14372

74) Yamaguchi K. et al. (2006) Biochem. Biophys. Res. Commun. **346**, 484-490

75) Miyagi T. et al. (1990) Jnp J. Cancer Res. **81**, 1286-1292

76) Ueno S. et al. (2006) J. Biol. Chem. **281**, 7756-7764

77) Wada T. et al. (2007) Oncogene **26**, 2483-2490

78) Nomura H. et al. (2006) Oncol. Res. **16**, 289-297

79) Tringali C. et al. (2008) Cell Death and Differ. **16(1),** 164-174

80) Yamanami H. et al. (2007) Cancer Sci. **98**, 299-307

81) Seyrantepe.V. et al. (2004) J. Biol. Chem. **279,** 37021-37029

82) Shiozaki K. et al (2009) J. Biol. Chem. **284(32),** 21157-21164

83) Gestblom C. et al. (1997) Am. J. Pathol. **150**, 107-117

84) Hoehner J.C.et al. (1996) Lab. Invest. **76**, 659-675

85) Gestblom C. et al (1999) Lab. Invest. **79**, 67-79

86) Cooper M.J. et al. (1990) Cell Growth Differ. **1**, 149-159

87) Gurney J.C. et al. (1997) J. Pediat. Hematol. Oncol. **19**, 428-432

88) Grovas A. et al. (1997) Cancer **80**, 2321-2332

89) Maris J.M. et al. (1999) J. Clin. Oncol. **7**, 2264-2279

90) Van Noesel M. M.et al. (2004) Gene **325**, 1-15

91) Brouder G. M. (2003) Nature Rew. Vol. 3, 202-216

92) Biedler J. L. et al. (1979) Gaslini (Genoa) **11**, 128-139

93) Ciccarone V. et al. (1989) Cancer Res. **49**, 219-225

94) Grady E. F. et al (1987) Cancer Res. **47**, 2931-2936

95) Biedler J. L. et al (1997) Lippincott-Raven Publ., 1053-1061

96) Ross R. A.et al.(1995) Cell Growth Differ. **6**, 449-456

97) Ross R.A et al. (2004) J. Natl. Cancer Inst. **96**, 1192-1193

98) Tsokos M. et al. (1987) Am. J. Pathol **128**, 484-496

99) Sugimoto T. et al. (1991) Int. J. Cancer **48(2),** 277-283

100) Walton J.D. et al. (2004) Neoplasia **6**, 838-845

101) Ross R.A. et al. (1983) J. Natl. Cancer Inst. **71**, 741-749

102) Kaneko Y. et al. (1987) Cancer Res. **47**, 311-318

103) Kaneko Y. et al. (1990) J. Clin. Oncol. **8**, 2005-2013

104) Look A.T. et al. (1984) N. Engl. J. Med. **311**, 231-235

105) Look A.T. et al. (1991) J. Clin. Oncol. **9**, 581-591

106) Schwab M. et al. (1983) Nature **305**, 245-248

107) Seeger R.C. et al. (1988) Prog. Clin. Biol. Res. **271**, 41-49

108) Brodeur G. M. et al. (1984) Science **224**, 1121-1124

109) Seeger R.C. et al. (1985) N. Engl. J. Med. **313**, 1111-1116

110) Slamon D.J. et al. (1986) Science **232**,768-772

111) Wenzel A. et al. (1991) EMBO J. **10**, 3703-3712

112) Nakagawara A. et al. (1992) Cancer Res. **52**, 1364-1368

113) Wada T.et al. (1993) Cancer **72**, 3346-3354

114) Cohn S.L. et al. (1991) Prog. Clin. Biol. Res. **366**, 21-27

115) Sivak L.E. et al. (1997) Oncogene **15**, 21-27

116) Fong C. T. et al. (1989) Proc. Natl. Acad. **86(10)**, 3753-7

117) Strieder V. et al. (2003) J. Biol. Chem. **278**, 2982-2989

118) Nakawara A. et al. (1994) Mol. Cell. Biol. **14**, 759-767

119) Acheson A. et al. (1995) Nature **374**, 450-453

120) Matsumoto K. et al. (1995) Cancer Res. **55**, 1798-1806

121) Eggert A. et al. (2000) Med. Pediatr. Oncol. **35**, 569-572

122) Ho R. et al. (2002) Cancer Res. **62**, 6462-6466

123) Yamashiro D. J. et al. (1996) Oncogene **12**, 37-41

124) Ryden M. et al. (1996) Br. J. Cancer **74**, 773-779

125) Bartscherer K. et al. (2008) EMBO Rep. **9**, 977–982

126) Mikels A. J. et al. (2006) Oncogene **25**, 7461–7468

127) Clevers H. (2006) Cell. **127**, 469–480

128) Kikuchi A. et al. (2009) Trends Cell. Biol. **19**, 119–129

129) Bhanot P. et al. (1996) Nature **382**, 225–230

130) Pinson K.I.et al. (2000) Nature **407**, 535–538

131) Tamai K. et al. (2000) Nature **407**, 530–535

132) Wehrli M. et al. (2000) Nature **407**, 527–530

133) Roszko I. et al. (2009) Semin. Cell Dev. Biol. **20**, 986–997

134) Wu J. (2009) Trends Cell. Biol. **19**, 295–305

135) He X. et al. (2004) Development **131**,1663–1677

136) Jin T. et al. (2008) Cell. Signal. **20**, 1697–1704

137) Kimelman D. (2006) Oncogene **25**, 7482–7491

138) Liu C. et al. (2002) Cell **108**, 837–847

139) Su Y. et al. (2008) Mol. Cell **32**, 652–661

140) Ikeda S. et al. (1998) EMBO J. **17**, 1371–1384

141) Zeng L. et al. (1997) Cell **90**, 181–192

142) Yanagawa S. et al. (1995) Genes Dev. **9**, 1087–1097

143) Wong H.C. et al. (2003) Mol. Cell **12**, 1251–1260

144) Chen W. et al. (2003) Science **301**, 1391–1394

145) Mao J. et al. (2001) Mol. Cell **7**, 801–809

146) Satoh J. et al. (2000) Neuropathology **20**, 113-123

147) Garcia-Perez J. et al. (1999) J Neurosci Res **57**, 261-270

148) Israsena N. et al. (2004) Dev. Biol **268**, 220-231

149) Ohira M. et al. (2000) Oncogene **19**, 4302-4307

150) Shimizu T. et al (2008) Mol. Cell. Biol **28(24)**; 7427-7441

151) Haegele L. et al (2003) Mol. Cell. Neurosci. **24(3)**; 696-708

152) Veh R. W. (1981) Perspect in inherited metabolic diseases vol 4,pp 71-109 edi Ermes, Milan

153) Chigorno V. et al. (1986), Anal. Biochem. **153**, 283

154) Goridis C. et al.(1992) Semin. Cell. Biol. **3(3),** 189-197

155) Hedgepeth C.M. et al. (1997) Dev. Biol. **185(1),** 82-91

156) Harbour J.W. et al. (2000) Nat. Cell. Biol **2(4)**, 65-67

157) Berthet C. et al. (2006) Cell Division **6**, 1-10

RINGARZIAMENTI

Oggi è il 10 Novembre 2010, fuori piove e io sono nella sala riunioni del LITA ed inizio a scrivere dei pensieri che mi ero ripromessa di evitare.

In un momento mi vengono in mente 1000 flashback di questi ultimi tre anni:

- ricordo l'inizio del dottorato.....ero spaventata perchè improvvisamente mi ritrovavo senza i miei compagni di sventura, con cui avevo fatto l'università e la tesi. Ma, per fortuna, è stato solo l'impatto iniziale, perchè poi ho conosciuto altre splendide persone: Silviuska, Pattonza, Giudi. Insieme abbiamo affrontato questi tre anni, le mitiche riunioni al Brallo, le risate e i momentacci perchè le cellule non fanno sempre quello che vogliamo ☺
- ricordo i miei due punti di riferimento al LITA: Cristina e Barbara, colleghe di lavoro con cui ho trascorso la maggior parte del tempo. Con loro mi sono confrontata, ho riso, scherzato, lavorato ed ottenuto grandi risultati (la Neu4 resta la migliore)
- ricordo i miei ex compagni di sventura: Alessandra Meini, Marco Lammendola, e Marco Piccoli, che sono sempre stati presenti nella mia vita e che, ormai, sono diventati degli amici
- ricordo il mio "guru", alias Danno, alias Davide, che ha saputo incoraggiarmi in momenti particolarmi, darmi ottimi consigni e fammi vedere il lato pratico della vita
- ricordo Toto e Lele, due ragazzi conosciuti per caso un'estate di 8 anni fà ed ormai diventati una sorta di fratelli acquisiti, perchè sono riusciti a conquistarmi con la loro tenerezza e le loro attenzioni
- ricordo la "zia Paola", amica da 14 anni ....un vero punto di riferimento, che nei prossimi due anni mi mancherà... Zia cambiano i luoghi, le persone, i momenti, ma noi ci siamo sempre ☺
- ricordo le mie "mitiche Tonne".....oooooh Tonne, sono stati 3 anni di cambiamenti, mi vengono in mente mille occasioni: il matrimonio di Sara (uno dei momenti più emozionanti e faticosi ☺ della mia vita) o il nostro viaggio a Stoccolma; ricordo le cene a casa di Silvia o i balletti sfrenati fatti durante una serata di Luglio; ricordo le serate passate al cinema con Anna, il nostro viaggio a Parigi, l'ultimo muro imbiancato ☺, o le mie fughe in negozio solo per farle un saluto veloce. Alt!!! Vi ricordate la sera passata nel locale di fronte al cinema le

giraffe?!? Il balletto mio e dell'anna sulle note della cuccarini?!?o il degenero che abbiamo creato?!?!Troppo troppo divertente.....

Tutti questi ricordi mi lasciano un sorriso sul volto, perchè è stato bello viverli.

Infine, mi viene in mente la mia famiglia:

- papà sempre pronto a spronarmi e a lanciarmi nella vita, ma che con uno sguardo mi fa capire che sto sbagliando
- la bassotta, sempre presente...che mi osserva quando sto in silenzio e rifletto, che capisce come sto da dei miei semplici gesti e che ritrovo ogni sabato pomeriggio seduta sul divano, sempre nella stessa posizione, insieme a Droga.
- Droga/B, la persona che ho voluto fin da piccola, che quando è arrivata mi ha reso felice, che mi conosce in ogni sfaccettatura, che mi fa ridere fino alle lacrime e che mi mancherà più di tutti

A tutte queste persone, e a quelle che mi sono dimenticata di nominare, dico grazie mille.

Fede